Accepted Manuscript

Tectonic evolution of the northern Austral-Magallanes basin in the Southern Patagonian Andes from provenance analysis

Vanesa Barberón, Gonzalo Ronda, Inés Aramendía, Rodrigo Suárez, Miguel E. Ramos, Maximiliano Naipauer, Christian Sue, Matías C. Ghiglione

PII: S0895-9811(19)30027-6

DOI: https://doi.org/10.1016/j.jsames.2019.102234

Article Number: 102234

Reference: SAMES 102234

To appear in: *Journal of South American Earth Sciences*

Received Date: 10 January 2019

Revised Date: 10 June 2019

Accepted Date: 13 June 2019

Tectonic evolution of the northern Austral-Magallanes basin in the Southern Patagonian Andes from provenance analysis

Vanesa Barberón[1*]; Gonzalo Ronda[1]; Inés Aramendía[2], Rodrigo Suárez[1]; Miguel E. Ramos[1]; Maximiliano Naipauer[3]; Christian Sue[4] and Matías C. Ghiglione[1]

[1)] Instituto de Estudios Andinos IDEAN (Universidad de Buenos Aires - CONICET), Buenos Aires, Argentina. *vanesabarberon@yahoo.com.ar

[2)] Instituto Patagónico para el Estudio de Ecosistemas Continentales, CCT-CONICET-CENPAT, Boulevard Brown 2915, Puerto Madryn, Chubut, Argentina

[3)] Instituto de Geocronología y Geología Isotópica INGEIS (Universidad de Buenos Aires - CONICET), Buenos Aires, Argentina.

[4)] Chrono-environnement, CNRS-UMR6249, Université de Bourgogne Franche-Comté, 16 route de Gray, 25030 Besançon cedex, France

Abstract

We studied the northern tip of the Austral-Magallanes basin in the Southern Patagonian Andes, between the Buenos Aires Lake and the Mayer River at 46º35' SL and 48º35' SL, respectively. Proposed objectives were: i) to differentiate Mesozoic-Cenozoic tectonostratigraphic units and, ii) to characterize the different deformational events that took place in the area linked to a variable regional geodynamic context. Sandstones provenance analysis was performed on the Aptian - Albian compressive retroarc deposits and Cenozoic foreland deposits. Studied samples were classified using tectonic discrimination diagrams which show: i) for Cretaceous rocks a dominant sediment source from a recycled orogen and, to a lesser extent, a dissected to transitional arc whereas ii) the Cenozoic rocks show a magmatic arc provenance. According to the performed analyses, the evolution of the northern sector of the Austral-Magallanes basin is proposed to include four tectonostratigraphic units related to: i) a Late Jurassic rift stage; ii) a Berriasian – Barremian thermal subsidence stage; iii) an Aptian – Albian compressive retroarc stage; and iv) a Miocene foreland stage *s.s*. The Late Cretaceous-Paleocene was

a time for compression and uplift, represented in the study zone by a paraconcordance/angular unconformity with an extended hiatus between Albian/Cenomanian rocks and the Eocene.

Keywords: Southern Patagonian Andes, geodynamics, tectonostratigraphic units, sedimentary petrography, provenance analysis.

1. Introduction

Development of the Austral-Magallanes basin (Figure 1) comprises Mesozoic-Cenozoic tectonic stages related to the passage from an extensional rift and thermal subsidence stage towards a foreland basin during compressional conditions in the Southern Patagonian Andes (SPA) in a subduction context (Wilson *et al.*, 1991; Robbiano *et al.*, 1996; Kraemer *et al.*, 2002; Franzese *et al.*, 2003; Rodríguez and Miller, 2005; Ghiglione *et al.*, 2010; Richiano *et al.*, 2012; Varela *et al.*, 2012).

The extensional stage involves a Jurassic rift related to the Gondwana breakup (Uliana *et al.*, 1989) represented along the SPA by the volcanic and volcaniclastic rocks from El Quemado Complex (Pankhurst *et al.*, 2000), and an Early Cretaceous thermal subsidence period represented by the well-sorted quartz-rich Springhill Formation followed by off-shore to shallow marine sequences from Río Mayer Formation (Richiano *et al*, 2012; Richiano, 2014; Aramendía *et al.*, 2018).

The change from thermal to tectonic subsidence occurred during the north to south diachronic onset of Andean uplift (Biddle *et al.*, 1986; Ramos, 1989; Wilson, 1991; Fosdick *et al.*, 2011), and is characterized by the appearance of more proximal sequences on top of the mainly pelitic-marine Río Mayer Formation. While first coarse sedimentation representing the onset of foreland sedimentation in the studied northern Austral-Magallanes basin consists of Aptian-Cenomanian continental sequences (Ghiglione *et al.*, 2015; Aramendía *et al.*, 2018), they are characterized by coarse-grained turbidites of late Albian-Cenomanian age in the southern sector (Figure 1; Kraemer and Riccardi, 1997; Fildani *et al.*, 2003; Fosdick *et al.*, 2011; Varela *et al.*, 2012).

A pronounced N-S Late Cretaceous segmentation represented one of the most important environmental and paleogeographic changes from the Austral-Magallanes foreland basin perspective: Whereas the northern region was uplifted during the Cenomanian and exposed to erosion during the rest of the Late Cretaceous-Paleocene (Ronda *et al.*, 2019), a 5800 m-thick marine sequence was deposited towards the south (Ghiglione *et al.*, 2009). Eocene-Miocene Andean synorogenic sequences are unevenly distributed, mainly in the northernmost sector in Guadal depocenter (Flint *et al.*, 1994; Encinas *et al.*, 2018), and in Río Turbio (Pearson *et al.*, 2012; Fosdick *et al.*, 2015). The Miocene, on the other hand, represents a continuous depocenter along the SPA foothills. These Miocene units reach the maximum thickness of 1000 m near Buenos Aires Lake (Ugarte, 1956; Flint *et al.*, 1994: Escosteguy *et al.*, 2001; Escosteguy *et al.*, 2003; Dal Molin and Colombo, 2003) diminishing to the south and east (Escosteguy *et al.*, 2003; Cuitiño and Scasso, 2010; Cuitiño *et al.*, 2012; 2015; 2019).

From the stated above, two characteristics distinguish the northern depocenter of the Austral-Magallanes basin from other sectors of the basin: (1) the earliest known foreland basin sediments for the onset of Andean deformation, Aptian-Albian in age; and (2) a Cenomanian-early Eocene period of non-deposition and erosion.

The aim of this work is to propose a consistent geodynamic model and definition of tectonostratigraphic stages representing these particularities. Summarized data from which our discussion and conclusions develops includes: sedimentary provenance analysis from detrital zircons (Ghiglione *et al.*, 2015) and sandstone petrography (Barberón *et al.*, 2015), sedimentary evolution (Cuitiño *et al.*, 2012, 2015, 2019; Aramendía *et al.*, 2018), kinematic indicators from fault analysis (Lagabrielle *et al.*, 2004; Diraison *et al.*, 2000: Barberón *et al.*, 2018), along with available geophysics datasets (Aramendía *et al.*, 2018) and structural studies (Ronda *et al.*, 2019; Ramos *et al.*, 2019).

2. Stratigraphic framework

A summary of the lithostratigraphic units for the studied area is presented in Figure 2, along with the location of the studied sedimentary profiles (Figures 3 and 4). The oldest exposed rocks are the metasediments of the Río Lácteo Formation (Bianchi, 1967) of Late Devonian to early Carboniferous age (Giacosa and Márquez, 2002; Augustsson *et al.*, 2006; Hervé *et al.*, 2007; Calderón *et al.*, 2016). The metamorphic basement lays unconformably under the volcanosedimentary successions of the El Quemado Complex (Riccardi, 1971). These rocks were dated at 157-153 Ma (Nullo *et al.*, 1978; Ramos, 1981; Pankhurst *et al.*, 2000; Iglesia Llanos *et al.*, 2003) and are related to the latest phase and the westernmost occurrence of the Jurassic silicic volcanism of Patagonia (stage V3 according to Pankhurst *et al.*, 2000; Figure 5 a-b)

The El Quemado Complex is overlain in erosive unconformity or paraconcordance by continental deposits, then followed by silicoclastic conglomerates and sandstones deposited in a marine shelf environment, both included within the Springhill Formation (Thomas, 1949), of Berriasian-Valanginian age (Ramos, 1979). The black marine shales of the Río Mayer Formation (Riccardi, 1971), of Hauterivian-Barremian age, were deposited in a transitional contact over the Springhill Formation, during a thermal subsidence stage (Arbe, 1986). In a transitional contact, deltaic deposits composed of green sandstones and shales are found, grouped in the Río Belgrano Formation (Ramos, 1979; Aguirre-Urreta and Ramos, 1981; Aramendía *et al.*, 2018) of Aptian age according to U-Pb dating on detrital zircons and tuffs (Ghiglione *et al.*, 2015). The Río Tarde Formation is overlaying, characterized by conglomerates and reddish sandstones in its lower member, interpreted as a high energy fluvial system (Arbe, 1986; Aramendía *et al.*, 2018). The upper member is dominated by reworked tuffs and sandstones deposited in a floodplain (Arbe, 1986). The Late Cretaceous is scarcely represented in the study area and corresponds to reddish and whitish continental deposits of the Cardiel Formation restricted to the Cenomanian (Russo and Flores, 1972).

The Eocene Posadas Basalt (Ramos, 2005) is assigned to the subduction of the Aluk-Farallon seismic ridge and the consequent development of an asthenospheric window between 53 and 43 Ma (Ramos and Kay, 1992; Ramos, 2005). Eocene times are also represented by alkaline basic intrusions of the Río Carbón Essexite (Giacosa and Franchi, 2001). Eocene sedimentary successions include metric-thick mudstones beds interbedded with centimetric-thick coal layers of the Río Lista Formation (Giacosa and Franchi, 2001). This sedimentary unit represents a continental paleoenvironment with numerous marshy deposits (Giacosa and Franchi, 2001).

Miocene sedimentation in the Austral-Magallanes basin initiates with an Atlantic marine transgression followed by continental sedimentary deposits. These marine deposits are assigned to El Chacay Formation in Posadas Lake area (Chiesa and Camacho, 1995; Parras *et al.,* 2012; Cuitiño *et al.*, 2015; 2019). Sedimentological studies by Cuitiño and Scasso (2010) near Estancia 25 de Mayo in the southern coast of Lago Argentino, redefined marine Patagonian beds, grouping these marine deposits in the Estancia 25 de Mayo Formation. In the rest of the basin Miocene's marine invasion is known as Centinela Formation (Escosteguy *et al.*, 2003). Overlying in transitional contact sandstones, mudstones and conglomerates continental deposits develop, assigned to the Santa Cruz Formation and the equivalent Río Zeballos Group in the Buenos Aires Lake area (Ugarte, 1956; Zambrano and Urien, 1970). The Neogene sedimentary succession is covered by late Miocene to Quaternary lava flows of the Meseta Lago Buenos Aires Formation (Sinito, 1980; Ramos and Kay, 1992; Gorring *et al.,* 1997; Ton-That *et al.,* 1999; Kay *et al.,* 2002) and the equivalent Belgrano Basalt (Riggi, 1957). Quaternary units are developed in the piedmont with glacial, fluvial, lacustrine and alluvial deposits (Giacosa and Franchi, 2001; Panza, 2002; Escosteguy *et al.*, 2003; Figure 2).

Following, we describe the sedimentary lithostratigraphic units where the provenance analyses were made, taking into account the lithology and thickness obtained on the sedimentary profiles (Figure 3) and the sedimentary environment. An important notice is that Springhill and Cardiel formations are scattered units, and are absent in our profiles.

2.1 Río Mayer Formation

The Río Mayer Formation is lithologically characterized by laminated black shales and very fine- to fine-grained sandstones interbedded with levels of fossil-rich sandstones with concretions (Figure 3). The top sector of each analyzed stratigraphic section is dominated by heterolithic stratification.

The registered thickness increased from north to south. In the western area of Posadas Lake (Figure 2) is around 80 meters (Figure 3), while for the Belgrano Lake area is 210 meters. Farther south, between the San Martín and Viedma lakes, the Río Mayer Formation is thicker, reaching 700 to 1000 meters (Riccardi, 1971; Nullo *et al.*, 1999).

This unit is interpreted as deposited in an inner marine platform passage to a shallow platform (Arbe, 2002). Aramendía *et al.* (2018) recognized upward coarsening arrangements representing a clear transition from marine to a transitional deltaic environment (Figure 3). To the south of the Austral-Magallanes basin, in outcrops located between San Martin and Argentino lakes, Richiano *et al.* (2012) identified three sections: (i) a lower section that corresponds to an external platform marine environment, (ii) a middle section with an external platform marine environment with deltaic influence, and (iii) an upper section that belongs to prodelta facies.

2.2 Río Belgrano Formation

The Río Belgrano Formation is composed mainly of green and gray color fine- to medium-grained sandstones, with thin pelitic intercalations and calcareous concretions levels. The middle part presents gray and black siltstones, and the section culminates with sandstones (Figure 3).

The Río Oro section (Figure 3) registered 40 meters of fine- to medium-grained greenish color sandstones interbedded with fine-grained conglomerates. In the Belgrano river (Figure 2), 117 meters of Río Belgrano Formation were measured, while in the Estancia Los Ñires and Arroyo Potranquitas (Figures 2 and 3) it reaches only 45 meters (Relañez, 2014; Ronda, 2015). The Río Belgrano Formation is interpreted as deposited in a wave dominated deltaic paleoenvironment where a delta front facies and a delta plain facies are recognized (Arbe, 2002). The medium-grained sandstones represent the continuity of the marine regression that begins with the upper section of the Río Mayer Formation in the Posadas Lake area. The stratigraphic relation between Río Belgrano and the underlying Río Mayer formation is pointing out the paleoenvironmental shift from an external shelf to a transitional environment close to the coastline (Aramendía *et al.*, 2018). This unit represents a particular regression of the northern sector of the Austral-Magallanes basin, developed from Pueyrredón Lake to the Arroyo Potranquitas to the south (Figure 3).

2.3 Río Tarde Formation

This lithostratigraphic unit is subdivided in two members (Ramos, 1979). The lower member is characterized by reddish medium-grained conglomerates interbedded with coarse- to very coarse-grained sandstones, with silicified wood remains towards the top as observed in the Río Oro profile (Figure 3). The sedimentary beds commonly present trough and planar cross-bedding, some siltstones beds are interbedded and contain wood remains. The medium-grained clast-supported conglomerates represent amalgamated channels that reach 25 meters thick (Aramendía *et al.*, 2018). Amalgamated conglomeradic channels are also interbedded with coarse- to very coarse-grained sandstones. The upper member is characterized by medium- to coarse grained sandstones with an important pyroclastic component. The upper member is more widespread and thicker in comparison with the lower member.

The thickness of the lower member varies between 55 and 93 meters around Posadas-Pueyrredón lakes (Ramos, 1979; Homovc, 1980; Cataldi, 2017). Better exposures for the upper member, between 320 and 356 meters are recorded along the Posadas and Belgrano lakes (Figure 5c; Ramos, 1979; Homovc, 1980).

The two members of the Río Tarde Formation represent two different fluvial paleoenvironments. The lower member of the Río Tarde Formation is interpreted as deposited by fluvial systems (Ramos, 1979; Arbe, 1986; Giacosa and Franchi, 2001). Aramendía *et al.* (2018) indicated that the presence of trough and planar cross-bedding structures could be associated with gravel bars in a braided fluvial system with scarce preservation of the floodplain. On the other hand, the rocks of the upper member correspond to floodplain deposits containing ash fall and lapilli (Figure 5c; Giacosa and Franchi, 2001; Cataldi, 2017).

2.4 Kachaike Formation

The Kachaike Formation consists of brown, medium- to coarse-grained tuffaceous sandstones with coal remains. Theses beds bear petrified trunks up to 1 meter in diameter and well-preserved fronds. In Estancia Los Ñires and Arroyo Potranquitas sections (Figure 3) the tuffaceous sandstones are interbedded with medium-grained sandstones with ammonites and bivalves. Levels of medium- to fine-grained gray tuffaceous sandstones reach-up 0.5-meter-thick, occasionally interbedded with reddish-brown sabulitic-grained sandstones levels and low angle stratification. Some sabulitic-grained moderate sorted sandstones are recognized and are characterized by pink colors subangular clasts with coal remains.

This unit is laterally correlated with the upper member of the Río Tarde Formation, based mainly on the lithology and stratigraphic relations (Ramos, 1979). The sedimentary environment interpreted by Rebasa (1982) consists of a deltaic paleoenvironment with deltaic plain at the base shifting to prodelta shales towards the top.

2.5 El Chacay Formation

The El Chacay Formation in the Río Belgrano section (Figure 4) initiates with massive fine – to medium-grained conglomerates composed of clasts of the Posadas Basalt. Overlying these conglomerates medium- to coarse-grained sandstones are often characterized by the presence of oysters, pectinids, bryozoans, brachiopods, echinoderms, turritellids. To the top of the succession structureless mudstones dominate and are interbedded with fine- to medium- grained sandstones with current ripple lamination. Below the transitional contact to the Santa Cruz Formation some different heterolithic bedding patterns arrangement (lenticular, wavy and flaser) are recognized.

The thickness registered west of Posadas Lake is 130 meters (Giacosa and Franchi, 2001; Vittore, 2002; Cuitiño *et al.*, 2015), and almost 270 meters in Río Belgrano section (Figure 4).

This unit represents the first marine transgression of the Atlantic Ocean that reached the cordilleran sector in the early Miocene (Cuitiño and Scasso, 2010). Cuitiño *et al.* (2015) interpreted a shallow marine environment dominated by tides that grades into an estuarine system with wave and fluvial influence that evidences a general transgressive-regressive cycle.

2.6 Santa Cruz Formation

The Santa Cruz Formation is distinguished on the field by their dark reddish color mudstones interbedded with medium-grained sandstones and siltstones (Figures 4 and 5c-d). In the studied area the Santa Cruz Formation reaches between 240 and 650 meters thick (Homovc, 1980; Ramos, 1979; Blisniuk *et al.*, 2005). Two sectors could be identified: i) structureless to laminated mudstones basal sector and ii) trough cross-bedded to horizontal stratification medium- to coarse-grained sandstones interbedded with structureless to horizontal laminated siltstones topping the whole section.

The Santa Cruz Formation is considered an equivalent to the Río Zeballos Group defined by Ugarte, 1956 in Buenos Aires Lake area. Río Zeballos Group includes all continental Miocene deposits represented by the Río Jeinemeni, Cerro Boleadoras and Río Correntoso formations (Escosteguy *et al.*, 2003). The Río Zeballos Group is restricted to the area between the Buenos Aires and Posadas lakes (Figures 2 and 6), while the Santa Cruz Formation extends south of the Austral-Magallanes Basin. Both units are interpreted to be synorogenic deposits (Ramos, 1989). The sedimentation of the Santa Cruz Formation occurs in a fluvial system, with an important pyroclastic participation toward the south (Cuitiño *et al.*, 2019). The continental coarsening upwards trend of the Santa Cruz Formation and the equivalent Río Zeballos Group is representing the regression of the early Miocene marine transgression related to the consequent Andean uplift westward.

3. Provenance analyses

We analyzed a total of 59 sandstones distributed in five stratigraphic sections (Figure 3), denominated from north to south (Figure 3): Río Oro, Veranada de Gómez, Río Belgrano, Estancia Los Ñires and Arroyo Potranquitas. Sandstones samples were classified based on their modal composition and linked to a regional tectonic context through ternary diagrams of tectonic discrimination (Dickinson and Suczek, 1979; Dickinson *et al.*, 1983; Ingersoll *et al.*, 1984). The reader is referred to Barberón *et al.* (2015) for more details in the methods and sample´s details, while a summary of the results follows, including additional samples and associations distinguished in groups according to the modal components.

Local pre-Cretaceous sources include Paleozoic rocks of Río Lácteo Formation and the Jurassic El Quemado Complex. In the case of a possible contribution from the Deseado Massif (Figure 1), lithological studies and detailed petrography were obtained from Giacosa *et al.* (2002). The analysis was carried on in the light clasts, the most abundant population. They were grouped according to each formation, in order to obtain an average value (Table 1).

An important scattering of the analyzed samples was obtained in Cretaceous rocks, while Cenozoic rocks resulted in a defined and bounded field, along with a low standard deviation (Figure 7). Several associations were distinguished according to the modal components: Groups A, B and C were identified taking into account the different proportions of minerals (Figure 7b; Table 1). These associations did not necessarily correspond to the same lithostratigraphic unit since the dispersion, in the case of the Cretaceous units analyzed, is significant.

In Group A Quartz is predominant, lithic fragments are found in a lesser proportion, and feldspars are scarce. Most of the samples from Río Mayer and Río Belgrano formations have preponderant metamorphic and sedimentary lithics, and are assembled in Group A (Figure 7b). Metamorphic lithics are composed of polycrystalline quartz and metaquartzite, and occasionally lithoclasts with lepidoblastic texture are recognized. This suggests a major contribution of metasedimentary basement rocks, while a volcanic input, even present, is subordinate (Figure 8).

Group B presents a proportional ratio of quartz-lithic fragments, while the proportion of feldspars is low. All the samples of the Río Tarde lower member and Kachaike formations are plotted in this field, indicating contribution of both, the basement source and the volcanic arc, in a variable range (Figure 7c). This mixed contribution is reflected in the distribution within various fields, including those of transitional recycled orogen, dissected and transitional arc fields (Figures 7a, b and d). This group includes some samples of Río Mayer and Río Belgrano formations, although a distinctive pattern overriding their distribution was not recognized.

Group C, which characterizes the Cenozoic record, is the most defined association, included within the transitional arc field. It comprises mostly lithic fragments and feldspars of the plagioclase type (Figures 7a, b and c), and low monocrystalline quartz content (Figures 7c and d). The volcanic lithics are the main lithologic type of fragments (Figure 8).

The average detrital modes for the Río Mayer and Río Belgrano formations are very close, with $Qm_{58}F_7Lt_{35}$ and $Qm_{48}F_{11}Lt_{41}$, respectively (Table 1; Figure7). For the Río Tarde and Kachaike formations, an average of $Qm_{35}F_{13}Lt_{52}$ was obtained, while for the

Miocene record the ratio between quartz and feldspars was inverted and the total lithic fragment content seemed slightly increased obtaining a mode of $Qm_{18}F_{38}Lt_{44}$.

Lower Cretaceous rocks present 50% of monocrystalline quartz, with values of lithic fragments not exceeding 40% and feldspars close to the remaining 10%. Towards the top of the Lower Cretaceous units, the proportion of monocrystalline quartz decreases, relatively increasing the proportion of lithics, and slightly increasing the number of feldspars (Figure 7d). For the Cenozoic rocks, the lithic and feldspar fragments are dominant with respect to the quartz (Figure 7d).

4. Tectonostratigraphic units

Combining the analysis of the lithostratigraphic units, the recognition of bounding discontinuities and unconformities, petrographic and provenance studies (Barberón *et al.*, 2015; Ghiglione *et al.*, 2015), and the information previously obtained on the brittle deformation and structural data (Aramendía *et al.*, 2018; Barberón *et al.*, 2018), we propose a new geodynamic evolution model for the northern sector of the SPA as synthesized in Figure 9. For further detailed information on structural domains and their evolution the reader is referred to Ronda *et al.* (2019) and Ramos *et al.* (2019).

4.1 Rift stage

This rift stage involves a basal lithostratigraphic unit named El Bello Formation (Escosteguy *et al.*, 2014) composed of conglomerates and sandstones of metasedimentary basement source (Figure 10a). The Jurassic volcanism follows, constituting the main syntectonic infill of grabens and halfgrabens. These extensional structures are ~N-S oriented, showing an E-W to NE-SW direction of extension (Figures 5a and 10a; Ramos, 1979; Sruoga *et al.*, 2010). Furthermore, a Jurassic transtensional component is proposed by Sruoga *et al.* (2010), at Sierra Colorada area (Figure 2).

The upper stratigraphic relations of this unit are variable, with transitional to sharp contacts, and concordance, paraconcordance, angular or erosive unconformities (Riccardi and Rolleri, 1980; Kraemer and Riccardi, 1997; Arbe, 2002; Etcheverría and Escosteguy, 2014). The diverse relations depend mostly on the relative position according to the extensional structures, related to the rift system. This explains why in the flexural margins a paraconcordance with the uppermost units is registered, while an angular unconformity in the active margins of the halfgrabens is produced (Kraemer and Riccardi, 1997; Nullo *et al.*, 1999).

The age of the extensional event is constrained between 157 and 153 Ma in the studied northern SPA. However, it is important to notice that stretching lasted longer in the southern SPA, where it continued until ~120 Ma, affecting up to Springhill and Río Mayer formations (Kraemer and Riccardi, 1997; Zerfass *et al.*, 2017). Magnitude of extension was also increasing towards the SW, developing quasi-oceanic crust in the Rocas Verdes basin along the Pacific archipelago (Calderón *et al.*, 2007, 2012, 2013).

Implications for a shorter extensional phase in the northern SPA, exhibiting less extension, contribute to paleogeographic effects in the ensuing retroarc basin: an early continentalization in the northern zone because the continental crust was less attenuated, and a quick response to the Aptian-Albian compression producing immediate uplift and migration of the orogenic front toward the east.

4.2 Thermal subsidence stage (sag)

Clastic sedimentation in the Austral-Magallanes basin begins with the Springhill Formation, including continental facies at its base, followed by marine deposits (Richiano *et al.*, 2016). The initial transgression is Tithonian at Argentino Lake area (Blasco *et al.*, 1979), but reached in the Berriasian-Valanginian the Posadas-Pueyrredon Lakes (Figure 10 b; Riccardi and Rolleri, 1980; Aguirre-Urreta and Ramos, 1981).

The major expansion of the basin took place with the black shales from Río Mayer Formation (Figure 10 c; Arbe, 1989, 2002), during the Barremian (Nullo *et al.*, 1999). Uplifted areas surrounding the marine basin were the SPA to the west, Aysén basin to the north, and the Deseado massif to the NE-E (Aguirre-Urreta and Ramos, 1981; Arbe, 1986, 2002).

Sandstones petrography analysis of the Río Mayer Formation shows typically low-grade metamorphic clasts, which could have come from the Deseado Massif (Figure 1), that was already exhumed in Early Cretaceous times (Giacosa *et al.*, 2010; Suarez *et al.*, 2019). The basement outcrops located in the western part of the Deseado Massif belong to La Modesta Formation (Moreira *et al.*, 2005, 2013), from the Silurian-Devonian. Since the basement of the SPA is always covered by the Jurassic (e.g. Figure 5a; Suarez *et al.*, 2019), and there is a lacking evidence for uplift and stratigraphic unroofing at this time, we consider that it did not contribute to a significant amount of basement sources.

As for the volcanic fragments, they correspond to acidic compositions and could be associated with contributions from the Chon Aike Formation distributed in the Deseado Massif, or linked to El Quemado Complex in the SPA. Both units are petrographically similar, only differing in their geochemical composition (Pankhurst *et al.*, 1998, 2000).

There is a significant spatial-temporal variation between the northern and southern SPA sectors of the basin in the sag stage. In the north, the Río Mayer Formation has a thickness of between 200 to 500 meters, with a Hauterivian-Barremian fossil age (Pöthe de Baldis, 1981; Ramos, 1982). In contrast, the southern outcrops register more than 700 meters and the age is up to Albian (Riccardi, 1971; Arbe and Hechem, 1984; Richiano *et al.*, 2012; Zerfass *et al.*, 2017).

From a deformational point of view, this stage presents an important paleobathimetric component controlled by the thermal subsidence postdating Jurassic rifting, which could have enhanced the flexural response as proposed by Giacosa *et al.* (2012), before the tectonic load of high surrounding blocks (Ghiglione *et al.*, 2015).

4.3 Compressive retroarc stage

There is an important Aptian change in sedimentation and paleobathymetric conditions with the onset of littoral and deltaic deposits of Río Belgrano Formation, which comprises the beginning of a regressive system (Figure 10d). U-Pb detrital zircons ages yielded a maximum depositional age of 122 Ma for the Río Belgrano Formation and the lower member of the Río Tarde Formation in the Posadas Lake area (Figure 2; Ghiglione *et al.*, 2015).

The Río Belgrano Formation represents a destructive deltaic environment with dominant wave action (Arbe, 1986) with the transitional passage from a marine environment (Río Mayer Formation) to a littoral high energy environment close to the coast

(Aramendía *et al.*, 2018). The progradation of this system was from E to W and ENE to WSW, considering a paleoshoreline oriented NNW (Figures 10d and 10e, Aguirre-Urreta and Ramos, 1981). The following, lower member of the Río Tarde Formation, on the other hand, has been interpreted as a continental high energy fluvial system with intercalated floodplain deposits (Giacosa and Franchi, 2001; Escosteguy *et al.*, 2003; Figure 10e).

The distribution of the U-Pb detrital zircon ages indicates a main contribution of the Jurassic volcanic stage V1 located in the North Patagonian massif and V2 from the Deseado massif, while there is a lack of ages from the El Quemado complex (V3) outcropping along the SPA. There are basement ages from Triassic, Paleozoic, Neoproterozoic and Mesoproterozoic (Ghiglione *et al.*, 2015). The sandstones of Río Belgrano Formation plot close to the apex of the monocrystalline quartz, depicting maturity and stability which is interpreted as coming from continental blocks. There is also a subordinate volcanic source according to the petrographic analyses. This source could have had the same origin as the underlying Río Mayer Formation, specifically in relation to the Jurassic volcanic rocks. It is then proposed that the main contribution came from elevated areas of the Deseado Massif to the east (Figure 1).

For Kachaike/Río Tarde formations, the analyzed samples plotted between the recycled orogen and the dissected to transitional arc fields (Figures 7a, b, c and d; Table 1). We interpret a contribution from both the basement source and the volcanic arc. The upper member of the Río Tarde Formation was dated at 112 Ma through U-Pb zircon ages in tuff (Ghiglione *et al.*, 2015), and it allows its correlation with the generalized volcanism in Patagonia (Figure 10f).

The Late Cretaceous is only represented by fine-grained deposits with tuffaceous intercalations of the Cardiel Formation (Figure 10g), and there is a hiatus in the sedimentation until the Eocene retroarc basalts (Figure 10h). Furthermore, existing evidence points out to active Andean deformation during the Late Cretaceous (Aramendía *et al.*, 2018; Gianni *et al.*, 2018 a, b; Ronda *et al.*, 2019). This fact suggests that the area was probably a positive element since the Cenomanian (Ghiglione *et al.*, 2015), and up to Eocene times.

There is nearly no sedimentary record from the Cenomanian to the Paleogene (Ramos, 1979; Arbe, 1989; Giacosa and Franchi, 2001; Ghiglione *et al.*, 2016), suggesting that this region of the SPA would have been a positive area during the Late Cretaceous.

This is an important issue, because it means that the northern sector was uplifted and acted as a major sedimentary source for the southern foreland basin depocenter beginning in Cenomanian time (Ronda *et al.*, 2019).

The reasoning to explain this early uplift includes a regional tectonic framework and local-regional stratigraphic-structural considerations:

By 115-112 Ma acceleration in the convergence rate between Farallón and South America plates led to subduction-related tectonic crustal shortening and thickening (Suárez *et al.*, 2009; Somoza and Ghidella, 2012). To the west of the Posadas Lake, contractional deformation is recognized, affecting the upper member of the Río Tarde Formation, with fault-propagation folds. Above, and in angular unconformity the Posadas Basalt and/or the El Chacay Formation are found in a subhorizontal position (Figures 5c and 10h; Suárez *et al.*, 2000; Aramendía *et al.*, 2018). Given the broad hiatus represented by this unconformity (Cenomanian-Eocene; Figure 5c), it is difficult to assign an age for the contractional deformation event that took place at some time during that interval. However, recently published anisotropy of magnetic susceptibility data (AMS) revealed that the deposition of the units of the Aptian-Albian age occurred in a region very close to the orogenic front, possibly in an environment of wedge top depozone (Aramendía *et al.*, 2018), together with the switch from Hauterivian-Barremian marine to Aptian-Cenomanian non-marine environments, suggest a regression due to tectonic causes (Aramendía *et al.*, 2018).

Kinematic reconstructed cross-sections of the area by Ronda *et al.* (2019) also sustain the onset of contractional deformation and initial basin positive inversion during Cenomanian times. In agreement with these studies, the evidence compiled and presented in this work indicates that the study area constituted an elevated area after the Cenomanian, possibly due to an early tectonic crustal shortening and thickening related to Andean uplift.

We propose that the folding affecting the Aptian to Cenomanian successions, very well represented in the outlet of the Furioso River and the SE wall of the Belgrano plateau, took place as part of a progress of the deformation that began in the Aptian-Albian when the continental synorogenic units are registered (Aramendía *et al.*, 2018), with the contribution of the tectonically elevated N and NE sectors. Towards the Cenomanian, there is a significant expansion of the volcanism that ends during the uplift of this sector of the basin that stands as a positive element up to Eocene times.

Additionally, it should be considered that in the southernmost sectors, where quasi-oceanic crust developed in the Rocas Verdes basin, the closure of this remaining ocean before the latest Cretaceous at around of 80 Ma (Calderón *et al.*, 2013) delayed the onset of the most important deformation pulses in the continental areas immediately located to the east (Ronda *et al.*, 2019).

5.4 Foreland stage

By the Eocene (Figure 10h), the retroarc volcanism of the Posadas Basalt is recorded in the SPA. This magmatism is considered a result of the collision of the Aluk-Farallón seismic ridge, ca. 52 Ma at 46º SL (Aragón *et al.*, 2013; Eagles and Jokat, 2014).

The Eocene-Miocene geodynamic scenario is characterized by oblique convergence of the Farallón and Nazca plates (Cande and Leslie, 1986; Pardo Casas and Molnar, 1987; Somoza and Ghidella, 2012), that would have caused strike-slip deformation in the basement domain, which is comparable to the current dynamics in the Northern Patagonian Andes (Cembrano and Hervé, 1993; Rosenau *et al.*, 2006; Cembrano and Lara, 2009; Georgieva *et al.*, 2016).

In the Miocene a renewed foreland stage began with the Burdigalian marine deposits of El Chacay Formation (Cuitiño *et al.*, 2015). This unit represents the Neogene Atlantic Ocean ingression (Ramos, 1979; Chiesa and Camacho, 1995) which advanced from the SE, continued to the W and NW (Cuitiño *et al.*, 2015). Afterwards, between 18 and 15 Ma the progradation of continental deposits of the Santa Cruz Formation are associated with the sedimentary supply produced by the synchronous tectonic uplift and erosion of the Andes (Ramos, 1989; Thomson *et al.*, 2001; Blisniuk *et al.*, 2005; Cuitiño *et al.*, 2015).

The results of petrographic sedimentary provenance in samples from these both units indicate a magmatic arc source, where lithic fragments and feldspar are predominant over the quartz content (Figures 7a, b and d). Also, the monomineralic fraction is dominated by plagioclase feldspar (Figure 7c). The origin of the lithic clasts is mainly volcanic, lesser metamorphic (Figure 8), along with scarce plutonic lithics. The samples exhibit several types of volcanic rock textures, both acidic and basic. For the early Miocene, a local contribution of the Posadas Basalt is inferred together with components derived from the magmatic arc located to the west. This stage corresponds to the Neogene foreland basin *sensu stricto*, receiving input from magmatic arc components to the west.

The Miocene deformation is conditioned by dominant strike-slip deformation in the SPA during the oblique subduction prior to the collision of the mid-ocean ridge segments (Lagabrielle *et al.*, 2007; Barberón *et al.*, 2018). Then, a brief extensional event registered by growth strata and kinematic indicators demonstrate an approximate E-W extension vector by the early Miocene (Figures 6a, 6c and 10i). Subsequently, the Chile Oceanic Ridge moved towards the South American margin, triggering compression at the basement front (Lagabrielle *et al.*, 2004). The synsedimentary folds and faults outcropping along the south margin of the Jeinemeni River (Lagabrielle *et al.*, 2004), and covering normal faults at the base of the cliff, show a sudden passage from extension to contraction (Figures 6b-c-d and 10j). These sequences are covered by the Cerro Boleadoras Formation, unit dated by U-Pb detrital zircon obtaining a maximum depositional age of 16.4 Ma (Folguera *et al.*, 2018), and it does not show deformation, marking a contrast in a short period of time where synextensional deposits are followed by a major phase of thrusts. The geodynamic context during the middle Miocene presents a warm and young oceanic crust approach of the Chilean seismic ridge, that is, a subduction with positive buoyancy and low subduction angle, indicating an episode of higher coupling between the South American and Nazca plates (Barberón *et al.*, 2018).

5. Concluding remarks

Mesozoic-Cenozoic sedimentation, paleoenvironments, and paleogeography, along the Austral-Magallanes Basin, were strongly influenced by a N-S-oriented segmentation, inherited from the widespread Jurassic rifting. Thus, the northern depocenter develops as a narrow and thinner basin, while southward, the basin expands and reaches higher thicknesses of lithostratigraphic units. By using sandstone provenance as a proxy to unravel the tectonostratigraphic stages, together with available geochronological and structural studies, a complex history of sedimentation and changes of the provenance's sources for the northern depocenter of the Austral-Magallanes Basin may be delineated. We identified a major change in the provenance of the basin from recycled orogen for the Cretaceous rocks to a strong signal of magmatic arc provenance for the Cenozoic rocks.

We defined a series of tectonostratigraphic stages since the opening of this sub-Andean depocenter up to last Andean uplift in Miocene times. Thus, we propose to include four tectonostratigraphic units related to i) Late Jurassic rift stage; ii) Berriasian – Barremian thermal subsidence stage; iii) Aptian – Albian compressive retroarc stage; and iv) Miocene foreland stage *s.s*. Strikingly, the Cenomanian-Eocene is not represented in the sedimentary record, depicting a major hiatus in this sector, due to its early uplift and erosion that sourced towards the southern depocenter.

Acknowledgements

We are very grateful to the people we met and who helped us in Bajo Caracoles and Lago Posadas. Special thanks to the park rangers of Perito Moreno (Lago Belgrano) and Patagonia National Parks, for their kindness and their logistical supports. Thanks to Sonia Quenardelle and the Geology Department of UBA-FCEN for provide the Microscope Laboratory and Swift Point counter. This is contribution R-288 of the Instituto de Estudios Andinos IDEAN Don Pablo Gröeber (UBA-CONICET).

References

Aguirre-Urreta, M.B., Ramos, V.A., 1981. Estratigrafía y Paleontología de la Alta Cuenca del Río Roble, provincia de Santa Cruz. 8° Congreso Geológico Argentino, Actas III: 101-132, San Luis.

Aragón, E., Pinotti, L., Fernando, D., Castro, A., Rabbia, O., Coniglio, J., Demartis, M., Hernando, I., Cavarozzi, C.E., Aguilera, Y.E., 2013. The Farallon-Aluk ridge collision with South America: Implications for the geochemical changes of slab window magmas from fore-to back-arc.Geoscience Frontiers. 4(4): 377-388.

Aramendía, I., Ramos, M.E., Ghiglione, M.C., Geuna, S., Cuitiño, J.I., 2018. A multidisciplinary study of the Lower Cretaceous marine to continental transition in the northern Austral-Magallanes basin and its geodynamic significance. Journal of South American Earth Sciences, 86: 54-69.

Arbe, H.A., 1986. El Cretácico de la Cuenca Austral: sus ciclos de sedimentación, Universidad de Buenos Aires, Tesis doctoral (inédito), 334 p., Buenos Aires.

Arbe, H.A., 1989. Estratigrafía y evolución sedimentaria del Cretácico en la Cuenca Austral, provincia de Santa Cruz. En: Chebli, G., Spalleti, L., (Eds.), Cuencas Sedimentarias Argentinas, Buenos Aires, 449-442.

Arbe, H.A., 2002. Análisis estratigráfico del Cretácico de la Cuenca Austral. En M.J. Haller (Ed.), Geología y Recursos Naturales de Santa Cruz. Relatorio del 15º Congreso Geológico Argentino. El Calafate, 1 (8): 103-128, Buenos Aires.

Arbe, H.A., Hechem, J.J., 1984. Estratigrafía y facies de depósitos marinos profundos del Cretácico Superior, Lago Argentino, Provincia de Santa Cruz. IX Congreso Geológico Argentino, Actas V, 7-41. Bariloche.

Augustsson, C., Münker, C., Bahlburg, H., Fanning, C.M., 2006. Provenance of late Palaeozoic metasediments of the SW South American Gondwana margin: a combined U–Pb and Hf-isotope study of single detrital zircons. Journal of the Geological Society, 163: 983-995.

Barberón, V., Ronda, G., Leal, P.R., Sue, C., Ghiglione, M.C., 2015. Lower Cretaceous provenance in the northern Austral basin of Patagonia from sedimentary petrography. J. S. Am. Earth Sci. 64, 498–510.

Barberón, V., Sue, C., Ghiglione, M., Ronda, G., Aragón, E., 2018. Late Cenozoic brittle deformation in the Southern Patagonian Andes: Record of plate coupling/decoupling during variable subduction?. Terra Nova, 30 (4): 296-309.

Bianchi, J.L., 1967. Informe preliminary acerca de los perfiles estratigráficos realizados en el sector occidental de la Cuenca Austral, durante las campañas 1964-65 y 1965-66. Yacimientos Petrolíferos Fiscales, (unpublished).

Biddle, K.T., Uliana, M.A., Mitchum, R.M., Fitzgerald, M.G., Wright, R.C., 1986. The stratigraphy and structural evolution of the central and eastern Magallanes Basin, southern South America. En: Allen, A. Homewood, P. (Eds), Foreland Basins, Blackwell Scientific Publications, London: Int. Assoc. Sediment. Spec. Pub., 8: 41-61.

Blasco, G., Nullo, F., Proserpio, C.A., 1979. Aspidoceras en Cuenca Austral, Lago Argentino, provincia de Santa Cruz. Revista de la Asociación Geológica Argentina, 34: 282-293.

Blisniuk P.M., Stern, L.A., Page Chamberlain, C., Idleman, B., Zeitler, P.K., 2005. Climatic and ecologic changes during Miocene surface uplift in the Southern Patagonian Andes. Earth and Planetary Science Letters, 230(1-2): 169-186.

Calderón M., Fildani, A., Hervé, F., Fanning, C.M., Weislogel, A., Cordani, U., 2007. Verdes basin, southern Patagonian Andes Late Jurassic bimodal magmatism in the northern sea-floor remnant of the Rocas, Journal of the Geological Society, 164: 1011-1022.

Calderón, M., Fosdick, J.C., Warren, C., Massonne, H.J., Fanning, C.M., Fadel Cury, L., Schwanethal, J., Fonseca, P.E., Galaz, G., Gaytán, D., Hervé, F., 2012. The low-grade Canal de las Montañas Shear Zone and its role in the tectonic emplacement of the Sarmiento Ophiolitic

Complex and Late Cretaceous Patagonian Andes orogeny, Chile. Tectonophysics, 524–525: 165–185.

Calderon, M., Prades, C. F., Herve, F., Avendaño, V., Fanning, C. M., Massonne, H. J., Theye, T., Simonetti, A., 2013. Petrological vestiges of the Late Jurassic-Early Cretaceous transition from rift to back-arc basin in southernmost Chile: New age and geochemical data from the Capitán Aracena, Carlos III, and Tortuga ophiolitic complexes. Geochemical Journal, 47(2): 201-217.

Calderón, M., Hervé, F., Fuentes, F., Fosdick, J.C., Sepúlveda, F., Galaz, G., 2016. Tectonic evolution of Paleozoic and Mesozoic Andean Metamorphic Complexes and the Rocas Verdes ophiolites in Southern Patagonia. In Springer Earth System Sciences MC Ghiglione (Ed) Geodynamic Evolution of the Southernmost Andes. 2:7-36.

Cande, S. C., Leslie, R. B., 1986. Late Cenozoic tectonics of the southern Chile trench. Journal of Geophysical Research-Solid Earth and Planets, 91(B1), 471-496, doi: 10.1029/JB091iB01p00471

Cataldi, L., 2017. Geología del sector norte de la Meseta Belgrano, provincia de Santa Cruz, Argentina. TFL, Facultad de Ciencias Exactas y Naturales, Universidad de Buenos Aires. Available at:http://digital.bl.fcen.uba.ar/download/seminario/seminario_nGEO001110_Cataldi.pdf

Cembrano, J., Hervé, F, 1993. The Liquine Ofqui fault zone: a major cenozoic strike slip duplex in the Southern Andes, paper presented at ISAG, ORSTOM Editions, Paris, Oxford, U.K.

Cembrano, J., Lara, L., 2009. The link between volcanism and tectonics in the southern volcanic zone of the Chilean Andes: A review. Tectonophysics, 471: 96–113

Cembrano, J., Hervé, F., Lavenu, A., 1996. The Liquiñe Ofqui fault zone: a long-lived intra-arc fault system in southern Chile. Tectonophysics, 259 (1-3): 55-66.

Chiesa, J.O., Camacho, H.H., 1995. Litoestratigrafía del Paleogeno marino en el noroeste de la provincia de Santa Cruz, Argentina. Academia Nacional Ciencias Exactas Físicas y Naturales. Monografía 11: 9-15. Buenos Aires.

Cuitiño, J.I., Scasso, R.A., 2010. Sedimentología y paleoambientes del Patagoniano y su transición a la formación Santa Cruz al sur del Lago Argentino, Patagonia Austral. Revista de la Asociación Geológica Argentina, 66 (3): 406–417.

Cuitiño, J.I., Pimentel, M.M., Ventura Santos, R., Scasso, R.A., 2012. High resolution isotopic ages for the early Miocene “Patagoniense” transgression in Southwest Patagonia: Stratigraphic implications. Journal of South American Earth Sciences, 38: 110-122.

Cuitiño, J.I., Santos, R.V., Muruaga, P.J. A., Scasso, R.A., 2015. Sr-stratigraphy and sedimentary evolution of early Miocene marine foreland deposits in the northern Austral (Magallanes) Basin, Argentina. Andean Geology, 42 (3): 364-385.

Cuitiño, J. I., Vizcaíno, S. F., Bargo, M. S., Aramendía, I., 2019. Sedimentology and fossil vertebrates of the Santa Cruz Formation (early Miocene) in Lago Posadas, southwestern Patagonia, Argentina. Andean Geology, 46(2).

Dal Molin, C.N., Colombo, F., 2003. Sedimentación neógena en la Cuenca del Río Zeballos y del Río Jenimeni (47º de Latitud Sur). Antepaís Patagónico, Argentina. Geogaceta 34: 139-142.

DeMets, C., Gordon, R.G., Argus, D.F., Stein, S., 1990. Current plate motions. Geophysical Journal International, 101 (2): 425-478.

Dickinson, W.R., Suczek, C., 1979. Plate tectonics and sandstone composition: American Association of Petroleum Geologists, Bulletin, v. 63, p. 2164–2182.

Dickinson, W.R., Beard, L.S., Brakenridge, G.R., Erjavec, J.L., Ferguson, R.C., Inman, K.F., Knepp, R.A., Lindberg, F.A., Ryberg, P.T., 1983. Provenance of North American Phanerozoic sandstones in relation to tectonic setting: Geological Society of America Bulletin, 94, 222-235.

Diraison, M., Cobbold, P.R., Gapais, D., Rossello, E.A., Le Corre, C., 2000. Cenozoic crustal thickening, wrenching and rifting in the foothills of the southermost Andes. Tectonophysics, 316: 91-119.

Eagles, G., Jokat, W., 2014. Tectonic reconstructions for paleobathymetry in Drake Passage. Tectonophysics, 611, 28-50.

Encinas, A., Folguera, A., Bechis, F., Finger, K.L., Zambrano, P., Pérez, F., Bernabé, P., Tapia, F., Riffo, R., Buatois, L., Orts, D., Nielsen, S.N., Valencia, V.V., Cuitiño, J., Oliveros, V., Lizet De Girolamo Del Mauro, Ramos, V.A, 2018. The Late Oligocene–Early Miocene Marine Transgression of Patagonia. In The Evolution of the Chilean-Argentinean Andes (pp. 443-474). Springer, Cham.

Escosteguy, L., Franchi, M., Dal Molin, C., 2001. Formación Ligorio Márquez (Paleoceno superior-Eoceno inferior) en el río Zeballos, provincia de SantaCruz, Argentina. 11° Congreso Latinoamericano de Geología, 3° Congreso Uruguayo de Geología. Montevideo.

Escosteguy, L., Dal Molín, C., Franchi, M., Geuna, S., Lapido, O., Genini, A., 2003. Hoja Geológica 4772-II, Lago Buenos Aires. Provincia de Santa Cruz. Instituto de Geología y Recursos Minerales, Servicio Geológico Minero Argentino. Boletín 339, 80 p., Buenos Aires.

Escosteguy, L., Geuna, S., Etcheverría, M., Franchi, M., 2014. Formación El Bello (nom. nov.), jurásico temprano de la cordillera Patagónica Austral, provincia de Santa Cruz. Revista de la Asociación Geológica Argentina, 71 (4): 575-584.

Etcheverría, M., Escosteguy, L., 2014. Nueva evidencia de contacto transicional entre El Complejo El Quemado y la Formación Springhill, Bahía de la Lancha, provincia de Santa Cruz. XIX Congreso Geológico Argentino, Actas en CD, Córdoba.

Fildani, A., Cope, T.D., Graham, S.A., Wooden, J.L., 2003. Initiation of the Magallanes foreland basin: Timing of the southernmost Patagonian Andes orogeny revised by detrital zircon provenance analysis. Geology, 31: 1081-1084.

Flint, S. S., Prior, D. J., Agar, S. M., Turner, P., 1994. Stratigraphic and structural evolution of the Tertiary Cosmelli Basin and its relationship to the Chile triple junction. Journal of the Geological Society, 151(2): 251-268.

Folguera, A., Encinas, A., Echaurren, A., Gianni, G., Orts, D., Valencia, V., Carrasco, G., 2018. Constraints on the Neogene growth of the central Patagonian Andes at the latitude of the Chile triple junction (45–47°S) using U/Pb geochronology in synorogenic strata. Tectonophysics, 744: 134-154.

Fosdick, J.C., Romans, B.W., Fildani, A., Bernhardt, A., Calderón, M., Graham, S.A., 2011. Kinematic evolution of the Patagonian retroarc fold-and-thrust belt and Magallanes foreland basin, Chile and Argentina, 51° 30' S. Geol. Soc. Am. Bull., 123: 1679–1698.

Fosdick, J. C., Grove, M., Graham, S.A., Hourigan, J.K., Lovera, O., Romans, B.W., 2015. Detrital thermochronologic record of burial heating and sediment recycling in the Magallanes foreland basin, Patagonian Andes. Basin Research, 27(4): 546-572.

Franzese, J., Spalletti, L., Pérez, I. G., Macdonald, D., 2003. Tectonic and paleoenvironmental evolution of Mesozoic sedimentary basins along the Andean foothills of Argentina (32–54º S). Journal of South American Earth Sciences, 16 (1): 81-90.

Georgieva, V. , Melnick, D., Schildgen, T.F., Ehlers, T.A., Lagabrielle, Y., Enkelmann, E., Strecker, M.R., 2016. Tectonic control on rock uplift, exhumation and topography above an oceanic-ridge collision – Southern Patagonian Andes (47°S), Chile. Tectonics, 35 (6): 1317-1341.

Ghiglione, M.C., Suarez, F., Ambrosio, A., Da Poian, G., Cristallini, E.O., Pizzio, M.F., Reinoso, R.M., 2009. Structure and evolution of the Austral basin fold–thrust belt, southern Patagonian Andes. Revista de la Asociación Geológica Argentina, 65: 215 - 226.

Ghiglione, M.C., Quinteros, J., Yagupsky, D., Bonillo-Martínez, P., Hlebszevtich, J., Ramos, V.A., Vergani, G., Figueroa, D., Quesada, S., Zapata, T., 2010. Structure and tectonic history of the foreland basins of southernmost South America. Journal of South American Earth Sciences, 29: 262-277.

Ghiglione, M. C., Naipauer, M., Sue, C., Barberón, V., Valencia, V., Aguirre-Urreta, B. and Ramos, V. A., 2015. U–Pb zircon ages from the northern Austral basin and their correlation with the Early Cretaceous exhumation and volcanism of Patagonia. Cretaceous Research, 55, 116-128.

Ghiglione, M. C., Ramos, V. A., Cuitiño, J., Barberón, V., 2016. Growth of the southern Patagonian andes (46–53 S) and their relation to subduction processes. In Growth of the Southern Andes (pp. 201-240). Springer, Cham.

Giacosa, R., Franchi, M., 2001. Hojas Geológicas 4772-III y 4772-IV Lago Belgrano y Lago Posadas, provincia de Santa Cruz. Servicio Geológico Minero Argentino, Boletín, 256.

Giacosa, R.E., Márquez, M.M., Panza, J.L., 2002. Basamento Paleozoico inferior del Macizo del Deseado. En: Haller, M.J. (ED.). Geología y Recursos Naturales de Santa Cruz. Relatorio XV Congreso Geológico Argentino, I-2: 33-44. Buenos Aires.

Giacosa, R.E., Márquez, M.M., 2002. El basamento paleozoico de la Cordillera Patagónica. En: Haller, M.J. (ED.). Geología y Recursos Naturales de Santa Cruz. Relatorio XV Congreso Geológico Argentino. El Calafate,I-3: 45-55. Buenos Aires.

Giacosa, R., Zubia, M., Sánchez, M., Allard, J., 2010. Meso-Cenozoic tectonics of the southern Patagonian foreland: Structural evolution and implications for Au-Ag veins in the eastern Deseado Region (Santa Cruz, Argentina). Journal of South American Earth Sciences, 30: 134-150.

Giacosa, R., Fracchia, D., Heredia, N., 2012. Structure of the Southern Patagonian Andes at 49°S. Geological Acta, 10: 265-282.

Gianni, G.M., Dávila, F.M., Echaurren, A., Fennell, L., Tobal, J., Navarrete, C., Quezada, P., Folguera, A., Giménez, M., 2018a. A geodynamic model linking Cretaceous orogeny, arc migration, foreland dynamic subsidence and marine ingression in southern South America. Earth-science reviews.

Gianni, G.M., Navarrete, C., Liendo, I., Díaz, M., Giménez, M.E., Encinas, A., Folguera, A., 2018b. Cretaceous Intraplate Contraction in Southern Patagonia: A Far-Field Response to Changing Subduction Dynamics?. Tectonics, 37(9): 2915-2937.

Gorring, M. L, Kay, S. M., Zeitler, P., Ramos, V. A., Rubiolo, D., Fernández, M. I., Panza, J. L., 1997. Neogene Patagonian plateau lavas: Continental magmas associated with ridge collision at the Chile Triple Junction. Tectonics, 16 (1): 1-17.

Hervé, F., Calderón, M., Faúndez, V., 2008. The metamorphic complexes of the Patagonian and Fuegian Andes. Geologica Acta, 6 (1): 43-53.

Hervé, F., Pankhurst, R.J., Fanning, C.M., Calderón, M., Yaxley, G.M., 2007. The South Patagonian batholith: 150 My of granite magmatism on a plate margin. Lithos, 97: 373–394.

Homovc, J.F., 1980. Estudio estratigráfico de la comarca ubicada en el margen septentrional de la meseta Belgrano, en la zona del Lago Posadas, Dpto. Río Chico, provincia de Santa Cruz. Trabajo final de licenciatura, Universidad de Buenos Aires. 2v, Buenos Aires.

Iglesia Llanos, P., Lanza, R., Riccardi, A.C., Geuna, S., Laurenzi, M.A., Ruffini, R. 2003. Palaeomagnetic study of the El Quemado complex and Marifil Formation, Patagonian Jurassic igneous province, Argentina. Geophys. J. Int. 154, 599-617.

Ingersoll, R.V., Bullard, T.F., Ford, R.L., Grimm, J.P., Pickle, J.D., Sares, S.W., 1984. The effect of grain size on detrital modes; a test of the Gazzi-Dickinson point-counting method. Journal of Sedimentary Research, 54 (1): 103-116.

Kay, S.M., Ramos, V.A., Gorring, M.L., 2002. Geochemistry of Eocene Plateau Basalts related to ridge collision in Southern Patagonia. XV Congreso Geológico Argentino. Actas 3: 60-65, Santa Cruz.

Kraemer, P.E., 1998. Structure of the Patagonian Andes. Regional balanced cross section at 508 S.L. Argentina. International Geology Review, 40: 896–915.

Kraemer, P.E., Riccardi A.C., 1997. Estratigrafía de la región comprendida entre los lagos Argentino y Viedma, Santa Cruz. Revista de la Asociación Geológica Argentina, 52 (3): 333-360.

Kraemer, P.E., Ploszkiewicz, J.V, Ramos, V.A., 2002. Estructura de la Cordillera Patagónica Austral entre los 46º y 52º S. En M.J. Haller (Ed.), Geología y Recursos Naturales de Santa Cruz. Relatorio del 15º Congreso Geológico Argentino. El Calafate, I (22): 353-364, Buenos Aires.

Lagabrielle, Y., Suárez, M., Rossello, E. A., Hérail, G., Martinod, J., Régnier, M., De la Cruz., R., 2004. Neogene to Quaternary evolution of the Patagonian Andes at the latitude of the Chile Triple Junction. Tectonophysics, 385: 211 – 241.

Lagabrielle, Y., Suarez, M., Malavieille, J., Morata, D., Espinoza, F., Maury, R. C., Bellon, H., 2007. Pliocene extensional tectonics in the Eastern Central Patagonian Cordillera: geochronological constraints and new field evidence. Terra Nova, 19(6): 413-424.

Moreira, P., González, P.D., Fernández, R., Echeveste, H., Schalamuk, I.A., Etcheverry, R., 2005. El basamento metamórfico de muy bajo a bajo grado de las estancias La Modesta y La Josefina, macizo del Deseado, provincia de Santa Cruz. Revista de la Asociación Geológica Argentina 60, 1, 49-63.

Moreira, P., Fernández, R., Hervé, F., Fanning, C.M., Schalamuk, I.A., 2013. Detrital zircons U-Pb SHRIMP ages and provenance of La Modesta Formation, Patagonia Argentina. Journal of South American Earth Sciences 47, 32–46.

Nullo, F.E., Proserpio, C.A., Ramos, V.A., 1978. Estratigrafía y tectónica de la vertiente este del Hielo Continental Patagónico, Argentina-Chile. VII Congreso Geológico Argentino, Neuquén, Actas, 1:455–470.

Nullo, F.E., Panza, J.L., Blasco, G., 1999. Jurásico y Cretácico de la Cuenca Austral. En R. Caminos (Ed.), Geología Argentina. Instituto de Geología y Recursos Minerales. Anales 29 (17-7): 528-535.

Pankhurst, R.J., Riley, T.R., Fanning, C.M., Kelley, S.P., 2000. Episodic silicic volcanism in Patagonia and the Antarctic Peninsula: chronology of magmatism associated with the break-up of Gondwana. Journal of Petrology, 41: 605–625.

Pankhurst, R.J., Weaver, S.D., Hervé, F., Larrondo, P., 1999. Mesozoic-cenozoic evolution of the north patagonian batholith in Aysén, southern Chile. J. Geol. Soc. 156 (4): 673–694.

Pankhurst, R., Leat, P.T., Sruoga, P., Rapela, C.W., Márquez, M., Storey, B.C., Ryley, T.R., 1998. The Chon Aike province of Patagonia and related rocks in west Antarctica: A silicic large igneous province. Journal of Volcanology and Geothermal Research, 81: 113–136.

Panza, J.L., 2002. La cubierta detrítica del Cenozoico superior. In M.J. Haller (Ed.), Geología y Recursos Naturales de Santa Cruz. Relatorio del XV Congreso Geológico Argentino El Calafate, I (17): 259-284, Buenos Aires.

Panza, J., Sacomanni, L., Cobos, J., 2003. Mapa Geológico de la Provincia de Santa Cruz. Instituto de Geología y Recursos Minerales, Servicio Geológico y Minero Argentino, Buenos Aires.

Pardo-Casas, F., Molnar, P., 1987. Relative motion of the Nazca (Farallon) and South American plates since Late Cretaceous time. Tectonics, 6(3): 233-248.

Parras, A., Dix, G.R., Griffin, M., 2012. Sr-isotope chronostratigraphy of Paleogene–Neogene marine deposits: Austral Basin, southern Patagonia (Argentina). Journal of South American Earth Sciences, 37: 122-135.

Pearson, N.J., Mángano, M.G., Buatois, L.A., Casadío, S., Raising, M.R., 2012. Ichnology, sedimentology, and sequence stratigraphy of outer-estuarine and coastal-plain deposits: Implications for the distinction between allogenic and autogenic expressions of the Glossifungites Ichnofacies. Palaeogeography, Palaeoclimatology, Palaeoecology, 333: 192-217.

Pöthe de Baldis, E.D., 1981. Análisis palinológico de muestras de la Hoja 52 a-b, Lago Pueyrredón, provincia de Santa Cruz. Servicio Geológico Nacional, (unpublished). Buenos Aires.

Ramos, M. E., Suárez, R., Boixart, G., Ghiglione, M., Ramos, V. A., 2019. The structure of the northern Austral Basin: Tectonic inversion of Mesozoic normal faults. Journal of South American Earth Sciences.

Ramos, V.A., 1979. Tectónica de la región del río y lago Belgrano, Cordillera Patagónica, Argentina. II Congreso Geológico Chileno, Actas I (B): 1-32, Santiago.

Ramos, V. A., 1981. Descripción geológica de la Hoja 55 a, Sierra de Sangra, Provincia de Santa Cruz. Servicio Geológico Nacional, (unpublished). Buenos Aires.

Ramos, V.A., 1982. Descripción geológica de las Hojas 53 a Monte San Lorenzo y 53 b, Monte Belgrano, Provincia de Santa Cruz. Servicio Geológico Nacional, (unpblished). Buenos Aires.

Ramos, V.A, 1989. Foothills structure in Northern Magallanes Basin, Argentina, American Association Petroleum Geologists, Bulletin 73 (7): 887-903, Tulsa.

Ramos, V.A., 2005. Seismic ridge subduction and topography: Foreland deformation in the Patagonian Andes. Tectonophysics, 399: 73–86.

Ramos, V.A., Kay, S.M., 1992. Southern Patagonian plateau basalts and deformation: backarc testimony of ridge collisions. Tectonophysics, 205: 261-282

Ramos, V.A., Niemeyer, H., Skarmeta, J., Muñóz, J., 1982. Magmatic evolution of the Austral Patagonian Andes. In: Cordani, H., Linares, E. (Eds.), Symposium on Magmatic Evolution of the Andes, Earth Sci. Review, 18: 411 – 443.

Rebasa, M., 1982. Análisis estratigráfico y paleoambiental de la Formación Kachaike, aflorante en la barranca epónima, provincia de Santa Cruz. Universidad de Buenos Aires, 52 p., unpublished, Buenos Aires.

Riccardi, A., 1971. Estratigrafía en el oriente de la Bahía de la Lancha, Lago San Martín, Santa Cruz, Argentina. Revista Museo de la Plata (nueva serie), 7, 61 p. La Plata.

Riccardi, A., Rolleri, E., 1980. Cordillera Patagónica Austral. En: Turner J. C. (Ed.): Segundo Simposio de Geología Regional Argentina, 2: 1173-1306. Academia Nacional de Ciencias. Córdoba.

Richiano, S.M. 2014. Lower Cretaceous anoxic conditions in the Austral basin, south-western Gondwana, Patagonia Argentina. Journal of South American Earth Sciences. 54: 37-46.

Richiano, S., Varela, A.N., Cereceda, A., Poiré, D.G., 2012. Evolución paleoambiental de la Formación Río Mayer, Cretácico Inferior, Cuenca Austral, provincia de Santa Cruz, Argentina. Latin American journal of sedimentology and basin analysis, 19 (1): 3-26.

Richiano, S., Varela, A.N., Poiré, D.G., 2016. Heterogeneous distribution of trace fossils across initial transgressive deposits in rift basins: an example from the Springhill Formation, Argentina. Lethaia, 49 (4): 524-539.

Riggi, J. C., 1957. Resumen geológico de la zona de los lagos Pueyrredón y Posadas, provincia de Santa Cruz. Revista Asociación Geológica Argentina, 12 (2): 65-97. Buenos Aires.

Robbiano, J.A., Arbe, H., Gangui, A., 1996. Cuenca Austral Marina. En Geología y Recursos Naturales de la Plataforma Continental Argentina (Ramos, V.A.; Turic, M.A.; editores). XIII Congreso Geológico Argentino, y III Congreso de Exploración de Hidrocarburos, Relatorio, p. 323-342. Buenos Aires.

Rodríguez, J., Miller, M., 2005. Cuenca Austral. En Frontera Exploratoria de la Argentina. VI Congreso de Exploración y Desarrollo de Hidrocarburos: 307-324.

Ronda, G., Ghiglione, M. C., Barberón V., Coutand, I., Tobal, J., 2019. Mesozoic - Cenozoic evolution of the Southern Patagonian Andes fold and thrust belt (47°-48°S): Influence of the Rocas Verdes basin inversion and onset of Patagonian glaciations. Tectonophysics, Doi: 10.1016/j.tecto.2019.05.009.

Ronda, G., 2015. Geología de las Sierras Baya y de Las Vacas, provincia de Santa Cruz, Argentina. Tesis de Grado, Facultad de Ciencias Exactas y Naturales. Universidad de Buenos Aires.

Rosenau, M., Melnick, D., Echtler, H., 2006. Kinematic constraints on intra-arc shear and strain partitioning in the southern Andes between 38°S and 42°S latitude. Tectonics, 25(4): TC4013.

Russo, A., Flores, M.A., 1972. Patagonia Austral Extrandina. En: Leanza, A. F. (Ed.): Segundo Simposio Geología Regional Argentina: 707- 725. Academia Nacional de Ciencias. Córdoba.

Somoza, R., Ghidella, M.E., 2012. Late Cretaceous to recent plate motions in western South America revisited. Earth and Planetary Science Letters, 331: 152-163.

Sinito, A. M., 1980. Edades geológicas, radimétricas y magnéticas de algunas vulcanitas cenozoicas de las provincias de Santa Cruz y Chubut. Rev. Asoc. Geol. Argent, 35, 332-339.

Sruoga, P., Japas, M.S., Salani, F., Kleiman, L.E., Rubinstein, N.A., 2010. Caldera La Peligrosa (47º15´ S, 71° 40´ O): un evento clave en la provincia silícea Chon Aike. Revista de la Asociación Geológica Argentina, 66(2): 368-380.

Suárez, R.J., González, P.D., Ghiglione, M.C., 2019. Tectonic evolution of the Paleozoic-Triassic basins from Patagonia: record of pre-Jurassic accretion and oceanward migration of the subduction zone. Journal of South American Earth Sciences, under review.

Suárez, M., De La Cruz, R., Aguirre-Urreta, B., Fanning, M., 2009. Relationship between volcanism and marine sedimentation in northern Austral (Aisén) Basin, central Patagonia: Stratigraphic, U-Pb SHRIMP and paleontologic evidence. Journal of South American Earth Sciences, 27: 309-325.

Suárez, M., De La Cruz, R., Bell, C. M., 2000. Timing and origin of deformation along the Patagonian fold and thrust belt. Geological Magazine, 137(4): 345-353.

Suarez, M., De La Cruz, R., 2000. Tectonics in the eastern central Patagonian Cordillera (45 30′–47 30′ S). Journal of the Geological Society, 157(5): 995-1001.

Thomas, C.R., 1949. Geology and petroleum exploration in Magallanes Province, Chile. American Association of Petroleum Geologists Bullettin, 33: 1553-1578.

Thomson, S.N., Herve, F., Stockhert, B., 2001. The Mesozoic-Cenozoic denudation history of the Patagonian Andes (southern Chile) and its correlation to different subduction processes. Tectonics, 20: 693–711.

Ton-That, T., Singer, B., Mörner, N. A., Rabassa, J., 1999. Datación de lavas basálticas por 40 Ar/39 Ar y geología glacial de la región del lago Buenos Aires, Provincia de Santa Cruz, Argentina. Revista de la Asociación Geológica Argentina, 54(4): 333-352.

Ugarte, F., 1956. El Grupo de Río Zeballos en el flanco occidental de la Meseta Buenos Aires. Revista de la Asociación Geológica Argentina, 11 (3): 202-216. Buenos Aires.

Uliana, M.A., Biddle, K.T., Cerdan, J., 1989. Mesozoic extension and the formation of Argentine sedimentary basins. In Extensional tectonics and stratigraphy of the North Atlantic margins. American Association of Petroleum Geologists Memoir, 46: 599-614.

Vittore, F.J., 2002. Estratigrafía y paleontología de las sedimentitas marinas de la Formación Centinela (Oligoceno tardío – Mioceno temprano), expuestas al sudoeste del lago Posadas, provincia de Santa Cruz, Argentina. Trabajo final de licenciatura, UNLPam, (unpublished), La Pampa.

Varela, A.N., Poiré, D.G., Martin, T., Gerdes, A., Goin, F.J., Gelfo, J.N., Hoffmann, S., 2012. U-Pb zircon constraints on the age of the Cretaceous Mata Amarilla Formation, Southern Patagonia, Argentina: its relationship with the evolution of the Austral Basin. Andean Geology, 39: 359-379.

Wilson, T.J., 1991. Transition from Back-Arc to Foreland Basin Development in the Southernmost Andes - Stratigraphic Record from the Ultima-Esperanza-District, Chile. Geological Society of America, Bulletin, 103: 98-111.

Zambrano, J., Urien, C., 1970. Geological outline of the basins in Southern Argentina and their continuation off the Atlantic shore. Journal of Geophysical Research, 75 (8): 1363-1396.

Zerfass, H., Ramos, V.A., Ghiglione, M.C., Naipauer, M., Belotti, H.J., Carmo, I.O., 2017. Folding, thrusting and development of push-up structures during the Miocene tectonic inversion of the Austral Basin, Southern Patagonian Andes (50° S). Tectonophysics, 699: 102-120.

Figure captions

Figure 1: Regional location of the studied area of the SPA in Patagonia, main morphostructural units and plate's boundaries (based on Ghiglione *et al.* 2010 and references therein). Convergence plate velocities based on De Mets *et al.* (1990). Red star refers to the actual position of the Chile Triple Junction (CTJ). References: LOFZ: Liquiñe-Ofqui Fault Zone; MFF: Magallanes-Fagnano Fault; NRS: North Scotia Ridge; LBA: Buenos Aires Lake; LPo: Posadas-Pueyrredón Lake; LBe: Belgrano Lake; LCa: Cardiel Lake; LSM: San Martín Lake; LVi: Viedma Lake; LAr: Argentino Lake; UEs: Última Esperanza; RTu: Río Turbio; MEs: Magallanes Strait.

Figure 2: Geological and structural map of the studied area, corresponding to the northern sector of the Austral basin and SPA. Modified from Panza *et al.* (2003) and Ronda *et al.* (2019).

Figure 3: Sedimentological profiles, located from north to south (right to left): Río Oro, Veranada de Gómez, Río Belgrano, Estancia Los Ñires and Arroyo Potranquitas (see location in Figure 2). In dashed red line are indicated the boundaries between Early Cretaceous lithostratigraphic units. Profiles are vertically correlated according to the base of Río Belgrano Formation. Grain size references above each profile: M: mudstone; mS: medium-grained sandstone; C: conglomerate. Kilometers above indicate the distance between each profile.

Figure 4: Continuation of Río Belgrano section, integrated profile including the Posadas Basalt, El Chacay Formation and the base of the Santa Cruz Formation.

Figure 5: (a) View toward the north of the Uñas range (see Figure 2 for location). Synextensional rocks of El Quemado Complex covering Río Lácteo Formation, that thickens towards a normal fault plane. (b) View to the south of the Uñas range, showing a

detail of west-dipping rocks of the El Quemado Complex which decrease their dip to the west. (c) Angular unconformity between the upper member (UM) of Río Tarde Formation and El Chacay Formation. (d) Miocene deposits in the Laguna La Oriental (Figure 2). The transitional contact between El Chacay and Santa Cruz formations is in white dotted line. Santa Cruz Formation strata with a decreasing dip towards the east are interpreted to be affected by progressive discordances.

Figure 6: (a) Northern shore of Lincoln River (Figure 2), where syntextensional growth strata were recognized within Río Jeinemeni Formation. The outcrop is approximately 100 meters wide; (b) Panoramic view toward the east of Cenozoic deposits in Jeinemeni River (Figure 2). In the bottom rocks of Río Jeinemeni Formation and to the top rocks of Cerro Boleadoras Formation. (c) Schematic evolution for the Miocene showing an extensional event in the lower Miocene and ensuing middle Miocene the main contractional phase. The extension is characterized by normal lystric faulting and synextensional growth strata. The stratigraphic colour code is the same as in Figure 2. (d) Middle Miocene compression is evidenced by the synorogenic Cerro Boleadoras Formation.

Figure 7: Ternary diagrams with the analyzed samples plotted by lithostratigraphic units and differentiated by the studied profiles: (a) QFL diagram proposed by Dickinson *et al.* (1983): Q: total quartz; F: feldspars; L: unstable lithics, (b) QmFLt diagram proposed by Dickinson *et al.* (1983): Qm: monocrystalline quartz; F: feldspars; Lt: total lithics. Groups A, B and C delimited (see text discussion), (c) Ternary monomineralic diagram QmPlgFk (Dickinson and Zucsek, 1979): Qm: monocrystalline quartz; Plg: plagioclase; Fk: potassium feldspar. (d) Average values plotted in the ternary diagrams QFL. Samples discriminate by lithostratigraphics units, from Early Cretaceous on the left to early Miocene on the right diagram. Polygons represent their standard deviation; refer to Table 1 for data.

Figure 8: S-N and vertical variation of lithic fragment composition within the analyzed sandstones samples in the studied profiles.

Figure 9: Synthesis of lithostratigraphic units and geological processes linked to the proposed tectonostratigraphic stages. References: (1) Lagabrielle *et al*. (2004); (2) Ramos *et al*. (1982), SPB: Southern Patagonian Batholith; (3) Pankhurst *et al*. (2000); (4) Hervé *et al*. (2008). Yellow star refers to the Farallón-Aluk ridge collision, and the red star refers to the Chile Oceanic Ridge (COR) collision to the South America plate.

Figure 10: (a) to (g) Block diagram showing the Mesozoic evolution of the northern end of the Austral basin for the (a) Late Jurassic, (b) Berriasian - Valanginian, (c) Hauterivian – Barremian, (d,e) Aptian, (f) Albian, and (g) Cenomanian. DM: Deseado Massif.

Figure 10 (continuation): (h) to (j) Block diagram showing the Cenozoic evolution of the northern end of the Austral basin for the (h) Eocene, (i) early Miocene, and (j) middle Miocene.

Table 1: Average values plotted in the ternary diagrams, by stratigraphic units, with their standard deviation (SD). Q: total quartz; F: feldspars; L: unstable lithics; Qm: monocrystalline quartz; F: feldspars; Lt: total lithics.

Formation		Q	F	L	Qm	F	Lt
Río Mayer	Average	60	7	33	58	7	35
n=10	SD	24,76	7,38	21,55	25,61	7,38	22,80
Río Belgrano	Average	51	11	38	48	11	41
n=35	SD	21,07	7,74	19,54	20,11	7,80	18,65
Río Tarde/Kachaike	Average	45	13	42	35	13	52
n=8	SD	17,30	12,04	15,96	15,65	11,9	19,46
El Chacay/Santa Cruz	Average	18	38	44	18	38	44
n=6	SD	5,03	6,66	8,26	5,00	6,66	8,34

TABLE 1

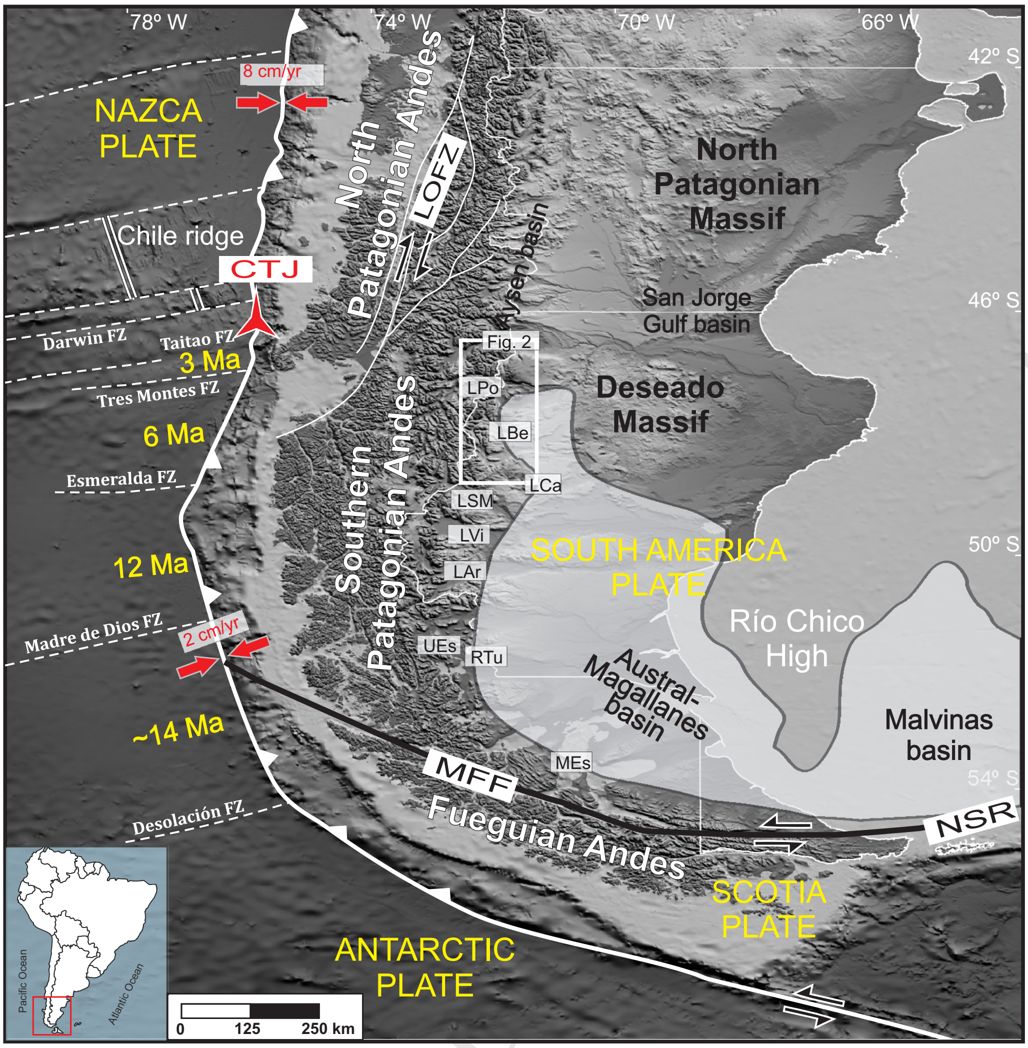
78° W
74° W
70° W
66° W
42° S
46° S
50° S
54° S
8 cm/yr
NAZCA PLATE
North Patagonian Andes
LOFZ
North Patagonian Massif
Aysen basin
Chile ridge
CTJ
San Jorge Gulf basin
Darwin FZ
Taitao FZ
3 Ma
Fig. 2
Tres Montes FZ
LPo
Deseado Massif
6 Ma
LBe
Esmeralda FZ
LCa
LSM
Southern Patagonian Andes
LVi
SOUTH AMERICA PLATE
12 Ma
LAr
Río Chico High
Madre de Dios FZ
2 cm/yr
UEs
RTu
Austral-Magallanes basin
~14 Ma
Malvinas basin
MEs
MFF
Desolación FZ
Fueguian Andes
NSR
SCOTIA PLATE
ANTARCTIC PLATE
Pacific Ocean
Atlantic Ocean
0
125
250 km

FIGURE 1

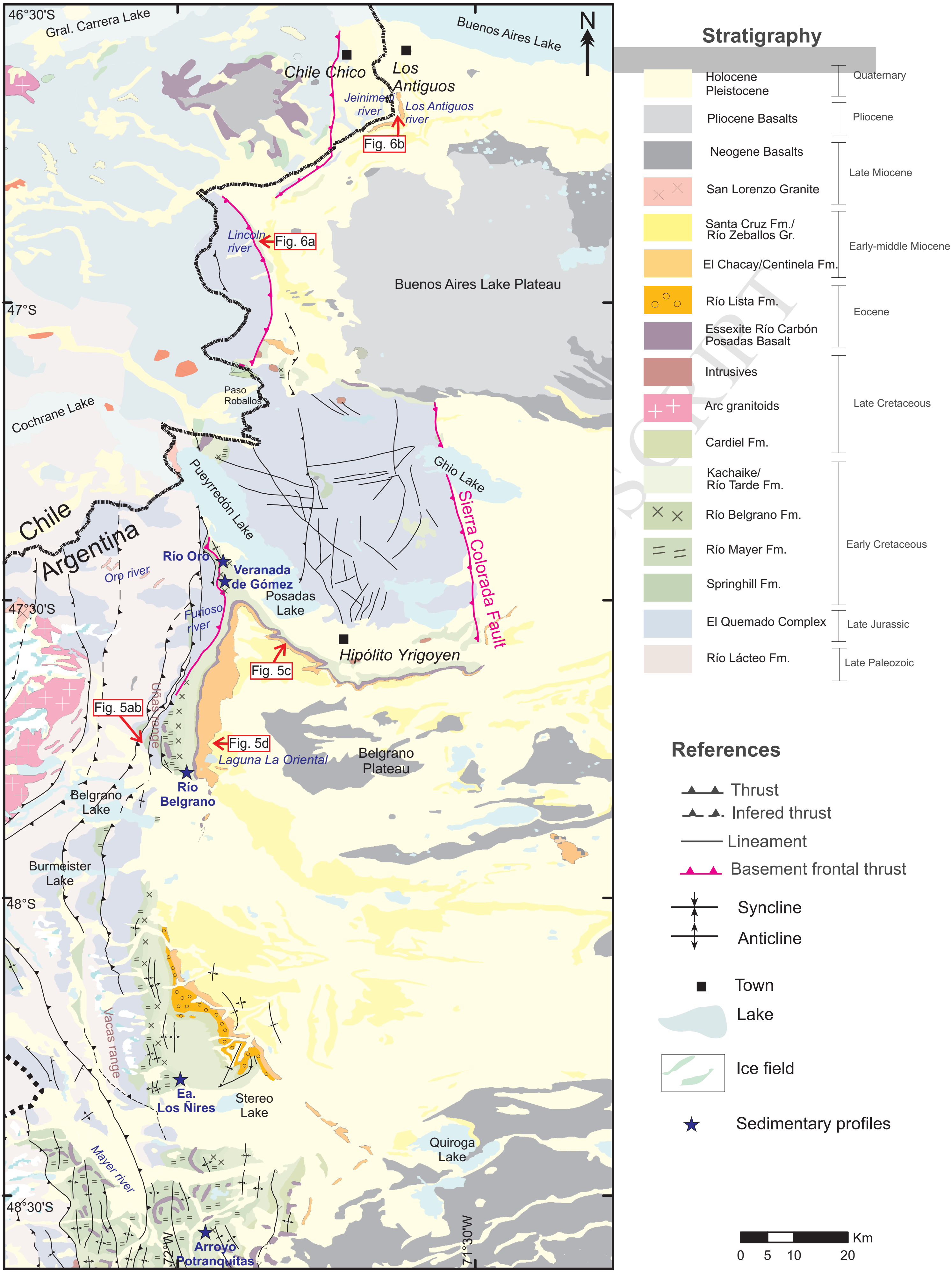

46°30'S
Gral. Carrera Lake
Buenos Aires Lake
N
Chile Chico
Los Antiguos
Jeinimeni river
Los Antiguos river
Fig. 6b
Lincoln river
Fig. 6a
Buenos Aires Lake Plateau
47°S
Paso Roballos
Cochrane Lake
Pueyrredón Lake
Ghio Lake
Sierra Colorada Fault
Chile
Argentina
Río Oro
Oro river
Veranada de Gómez
Posadas Lake
47°30'S
Furioso river
Hipólito Yrigoyen
Fig. 5c
Fig. 5ab
Uñas range
Fig. 5d
Laguna La Oriental
Belgrano Plateau
Río Belgrano
Belgrano Lake
Burmeister Lake
48°S
Vacas range
Ea. Los Ñires
Stereo Lake
Quiroga Lake
Mayer river
48°30'S
72°W
71°30'W
Arroyo Potranquitas
Stratigraphy
Holocene
Pleistocene
Quaternary
Pliocene Basalts
Pliocene
Neogene Basalts
Late Miocene
San Lorenzo Granite
Santa Cruz Fm./
Río Zeballos Gr.
Early-middle Miocene
El Chacay/Centinela Fm.
Río Lista Fm.
Eocene
Essexite Río Carbón
Posadas Basalt
Intrusives
Late Cretaceous
Arc granitoids
Cardiel Fm.
Kachaike/
Río Tarde Fm.
Río Belgrano Fm.
Río Mayer Fm.
Early Cretaceous
Springhill Fm.
El Quemado Complex
Late Jurassic
Río Lácteo Fm.
Late Paleozoic
References
Thrust
Infered thrust
Lineament
Basement frontal thrust
Syncline
Anticline
Town
Lake
Ice field
Sedimentary profiles
Km
0 5 10 20

FIGURE 2

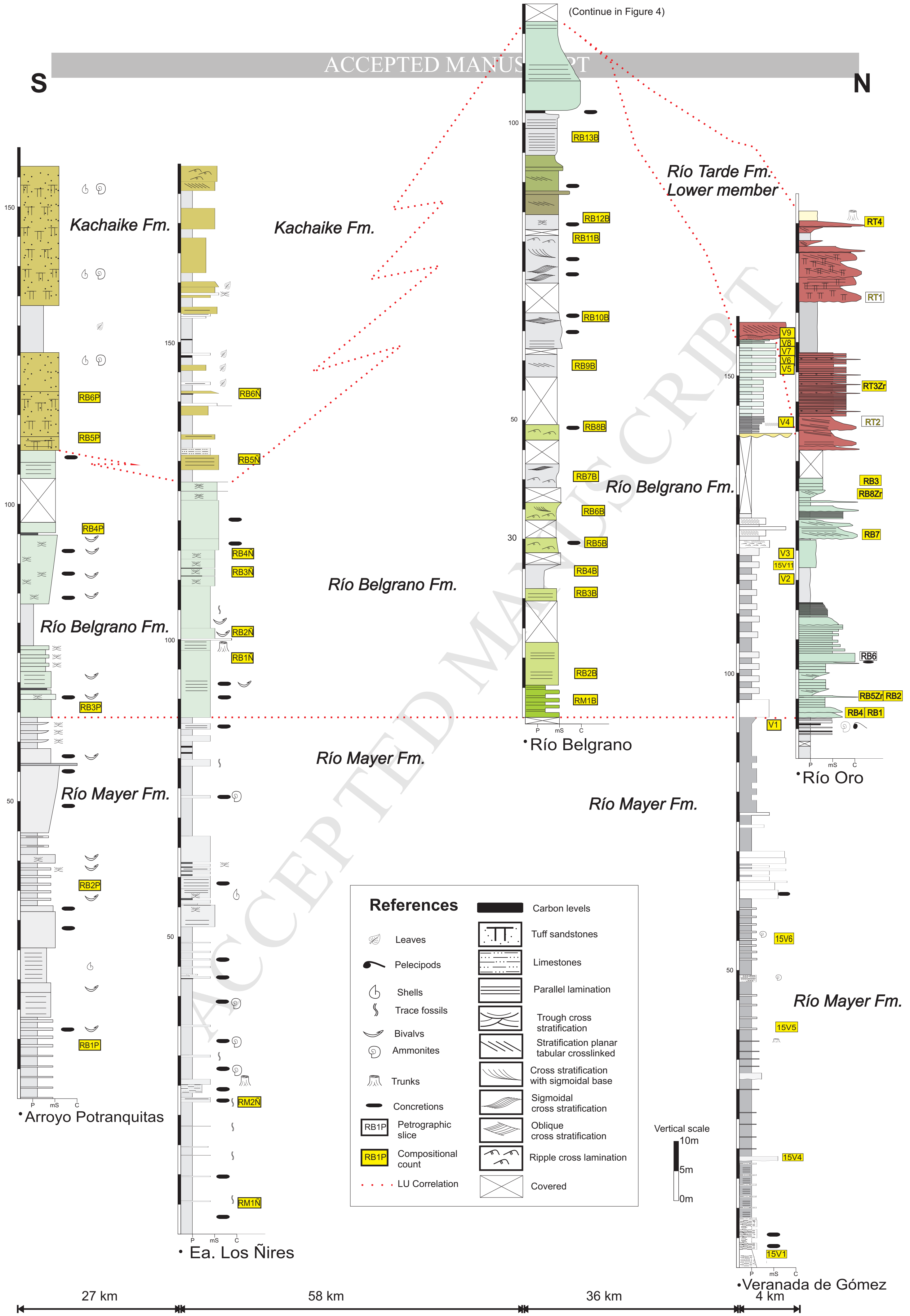
(Continue in Figure 4)
S
N
Kachaike Fm.
Kachaike Fm.
Río Tarde Fm.
Lower member
Río Belgrano Fm.
Río Belgrano Fm.
Río Belgrano Fm.
Río Mayer Fm.
Río Mayer Fm.
Río Mayer Fm.
Río Mayer Fm.
RB13B
RB12B
RB11B
RB10B
RB9B
RB8B
RB7B
RB6B
RB5B
RB4B
RB3B
RB2B
RM1B
RB6P
RB5P
RB4P
RB3P
RB2P
RB1P
RB6Ñ
RB5Ñ
RB4Ñ
RB3Ñ
RB2Ñ
RB1Ñ
RM2Ñ
RM1Ñ
RT4
RT1
RT3Zr
RT2
RB3
RB8Zr
RB7
RB6
RB5Zr RB2
RB4 RB1
V9
V8
V7
V6
V5
V4
V3
15V11
V2
V1
15V6
15V5
15V4
15V1
150
100
50
30
P mS C
Arroyo Potranquitas
Ea. Los Ñires
Río Belgrano
Río Oro
Veranada de Gómez
References
Carbon levels
Leaves
Tuff sandstones
Pelecipods
Limestones
Shells
Parallel lamination
Trace fossils
Trough cross stratification
Bivalvs
Stratification planar tabular crosslinked
Ammonites
Cross stratification with sigmoidal base
Trunks
Sigmoidal cross stratification
Concretions
Petrographic slice
Oblique cross stratification
Compositional count
Ripple cross lamination
LU Correlation
Covered
Vertical scale
10m
5m
0m
27 km
58 km
36 km
4 km

FIGURE 3

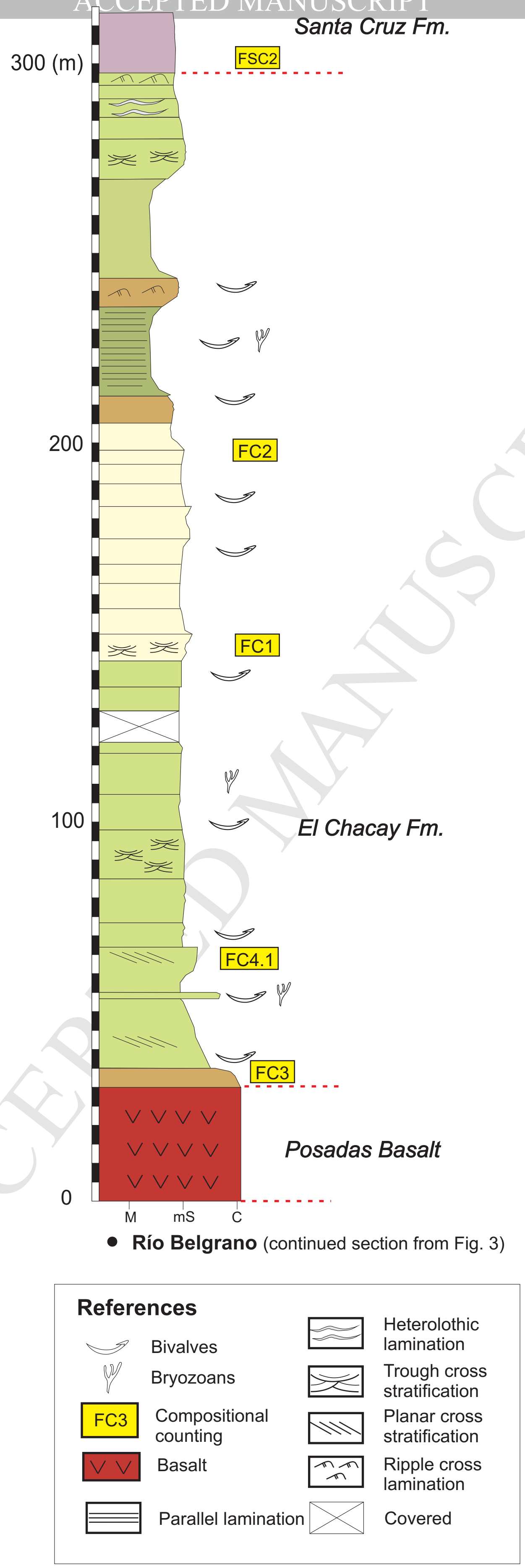

Santa Cruz Fm.
300 (m)
FSC2
200
FC2
FC1
100
El Chacay Fm.
FC4.1
FC3
Posadas Basalt
0
M
mS
C
● Río Belgrano (continued section from Fig. 3)
References
Bivalves
Bryozoans
FC3
Compositional counting
Basalt
Parallel lamination
Heterolothic lamination
Trough cross stratification
Planar cross stratification
Ripple cross lamination
Covered

FIGURE 4

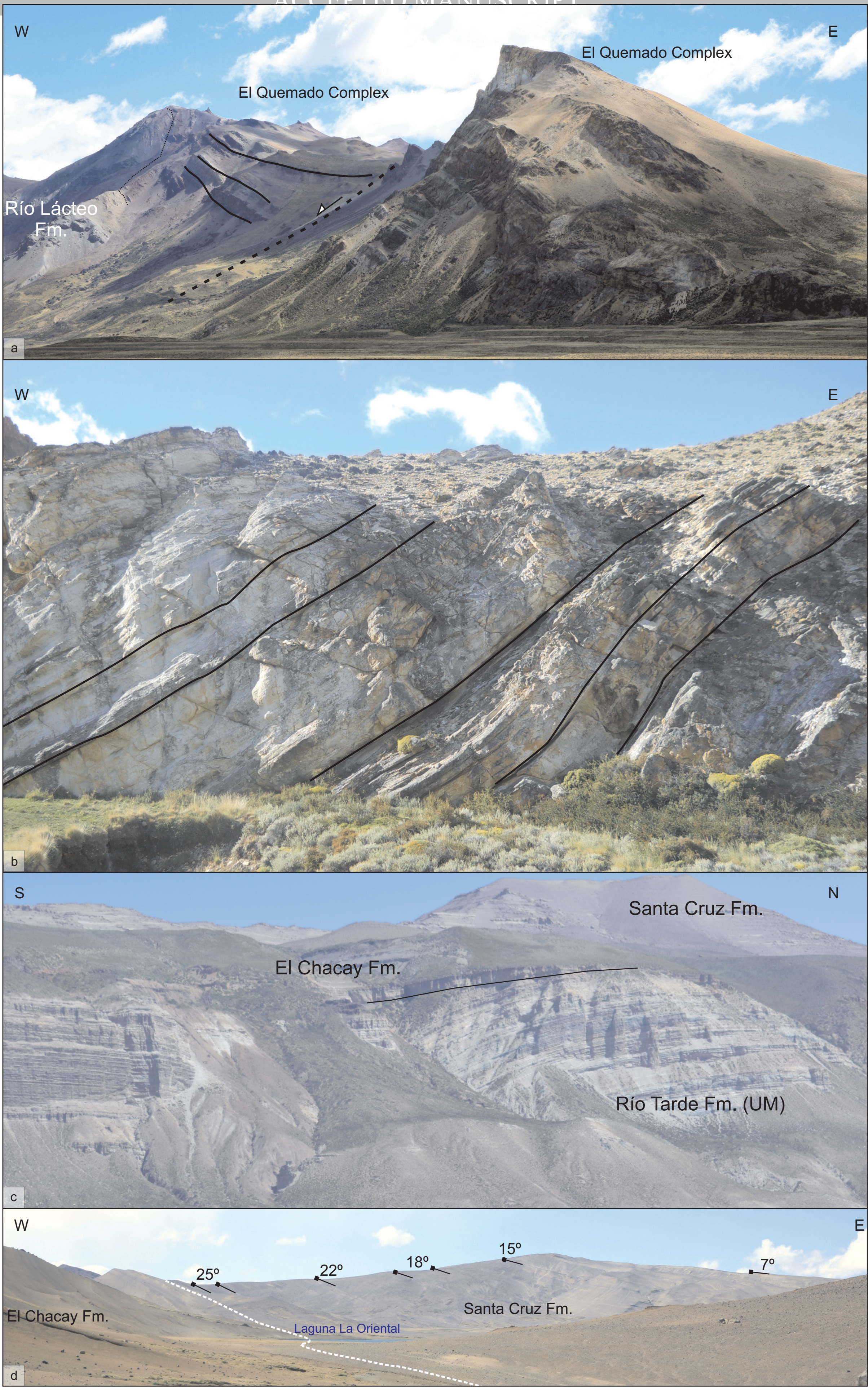
W
E
El Quemado Complex
El Quemado Complex
Río Lácteo Fm.
a
W
E
b
S
N
Santa Cruz Fm.
El Chacay Fm.
Río Tarde Fm. (UM)
c
W
E
25º
22º
18º
15º
7º
El Chacay Fm.
Santa Cruz Fm.
Laguna La Oriental
d

FIGURE 5

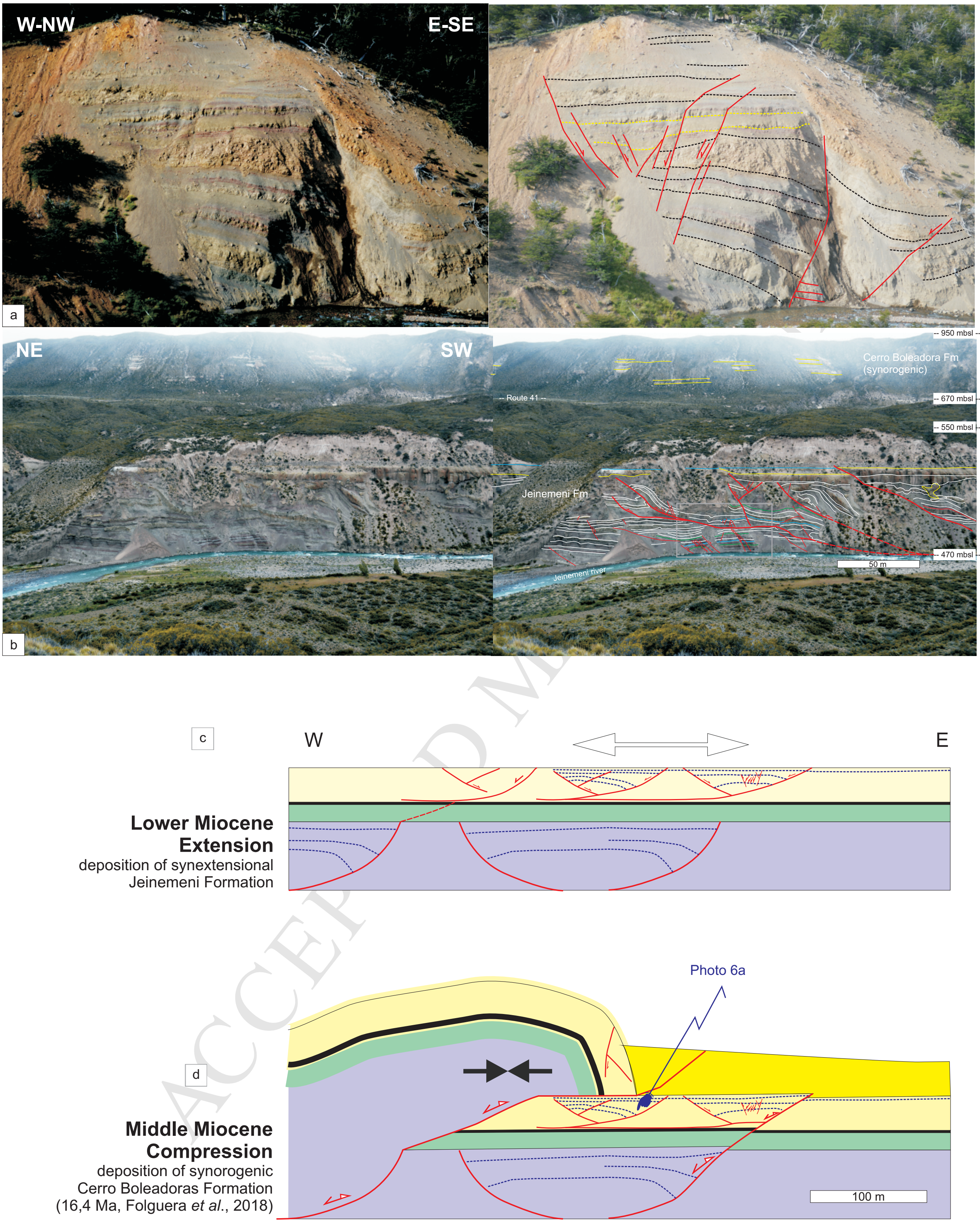
W-NW
E-SE
a
NE
SW
b
950 mbsl
Cerro Boleadora Fm
(synorogenic)
Route 41
670 mbsl
550 mbsl
Jeinemeni Fm
470 mbsl
50 m
Jeinemeni river
c
W
E
Lower Miocene
Extension
deposition of synextensional
Jeinemeni Formation
Photo 6a
d
Middle Miocene
Compression
deposition of synorogenic
Cerro Boleadoras Formation
(16,4 Ma, Folguera et al., 2018)
100 m

FIGURE 6

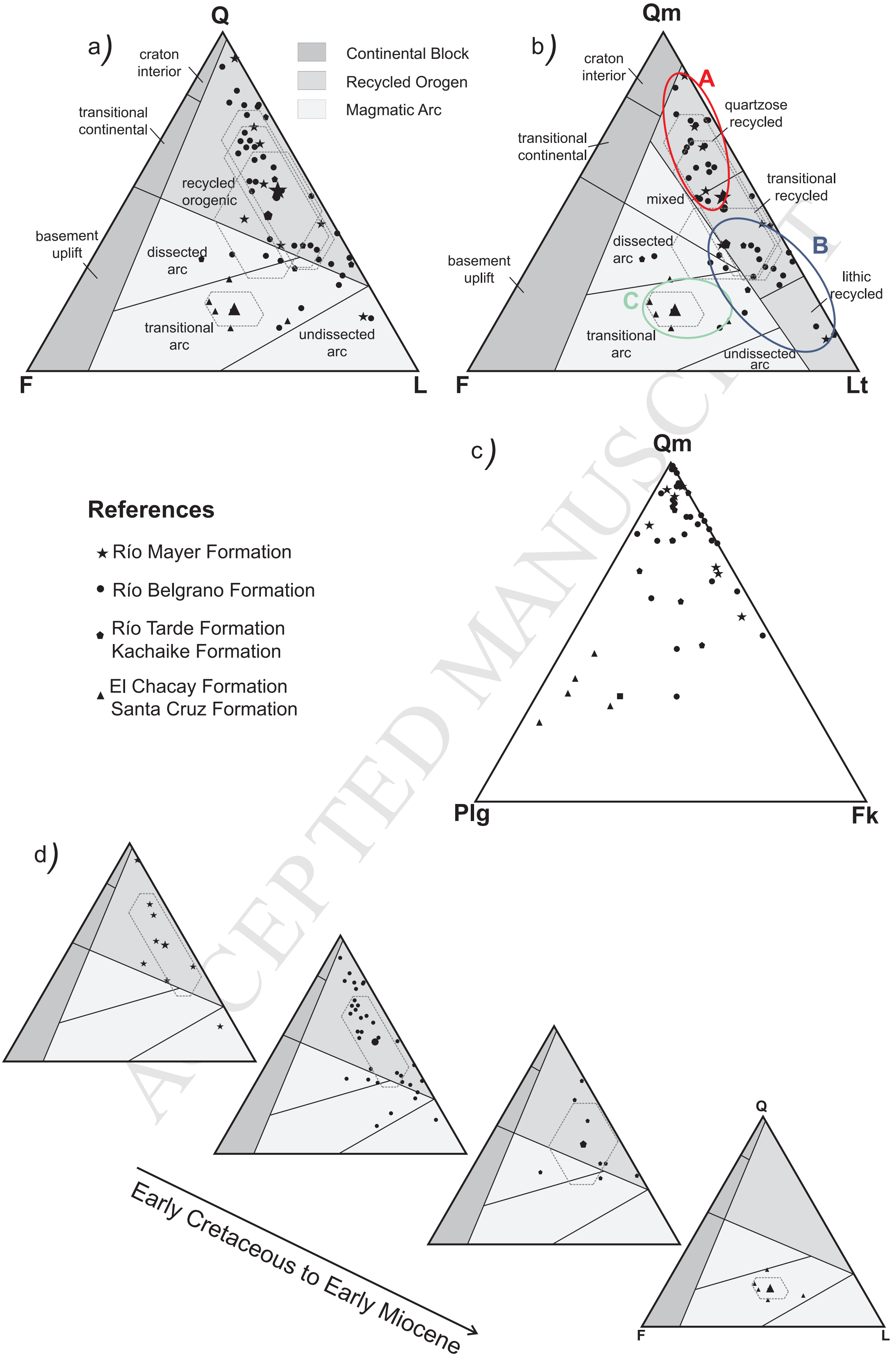
a)
Q
F
L
craton interior
transitional continental
recycled orogenic
basement uplift
dissected arc
transitional arc
undissected arc
Continental Block
Recycled Orogen
Magmatic Arc
b)
Qm
F
Lt
craton interior
transitional continental
quartzose recycled
transitional recycled
mixed
dissected arc
basement uplift
lithic recycled
transitional arc
undissected arc
A
B
C
c)
Qm
Plg
Fk
References
Río Mayer Formation
Río Belgrano Formation
Río Tarde Formation
Kachaike Formation
El Chacay Formation
Santa Cruz Formation
d)
Q
F
L
Early Cretaceous to Early Miocene

FIGURE 7

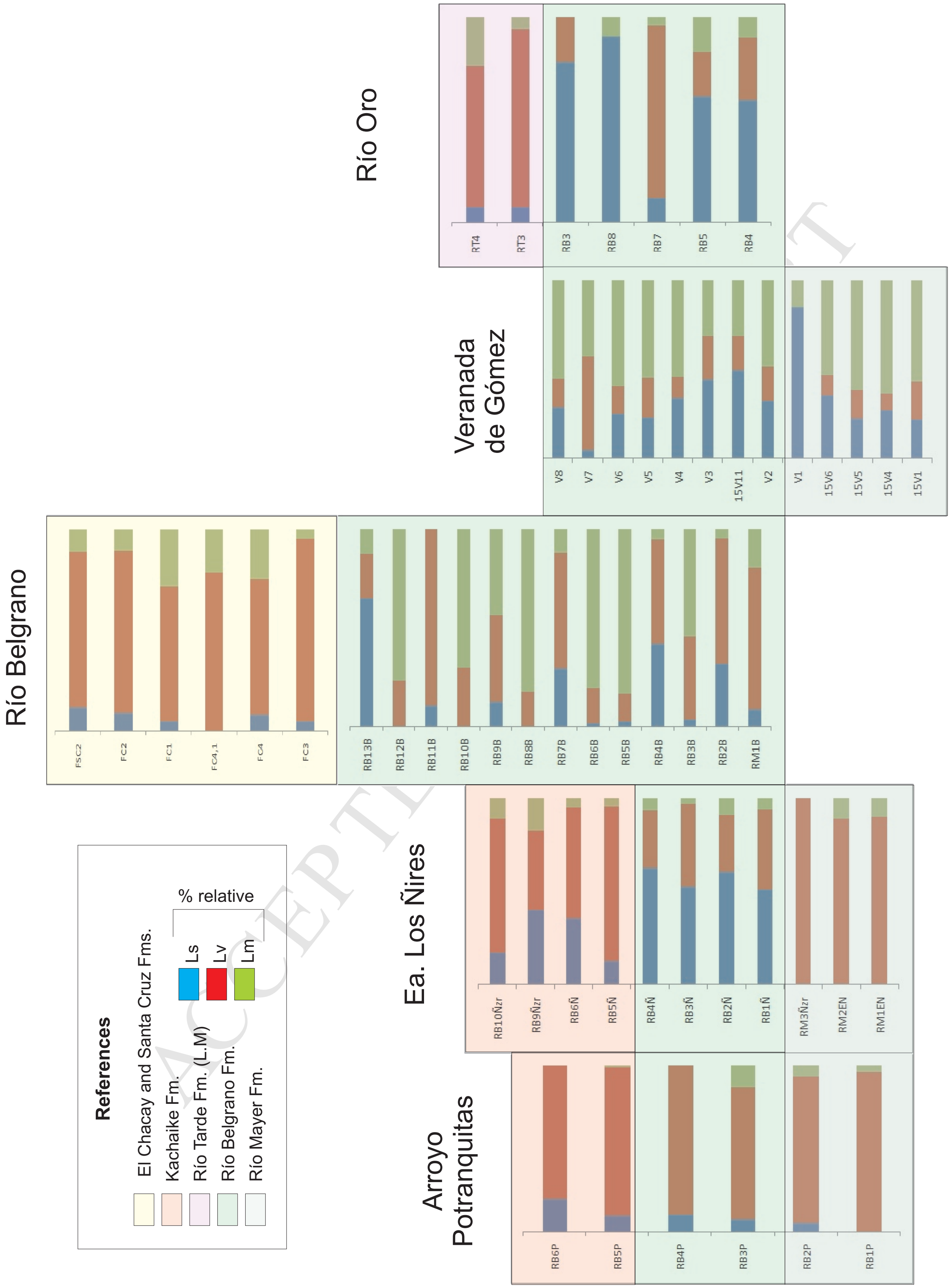

Río Oro
RT4
RT3
RB3
RB8
RB7
RB5
RB4
Veranada de Gómez
V8
V7
V6
V5
V4
V3
15V11
V2
V1
15V6
15V5
15V4
15V1
Río Belgrano
FSC2
FC2
FC1
FC4,1
FC4
FC3
RB13B
RB12B
RB11B
RB10B
RB9B
RB8B
RB7B
RB6B
RB5B
RB4B
RB3B
RB2B
RM1B
Ea. Los Ñires
RB10Ñzr
RB9Ñzr
RB6Ñ
RB5Ñ
RB4Ñ
RB3Ñ
RB2Ñ
RB1Ñ
RM3Ñzr
RM2EN
RM1EN
Arroyo Potranquitas
RB6P
RB5P
RB4P
RB3P
RB2P
RB1P
References
El Chacay and Santa Cruz Fms.
Kachaike Fm.
Río Tarde Fm. (L.M)
Río Belgrano Fm.
Río Mayer Fm.
Ls
Lv
Lm
% relative

FIGURE 8

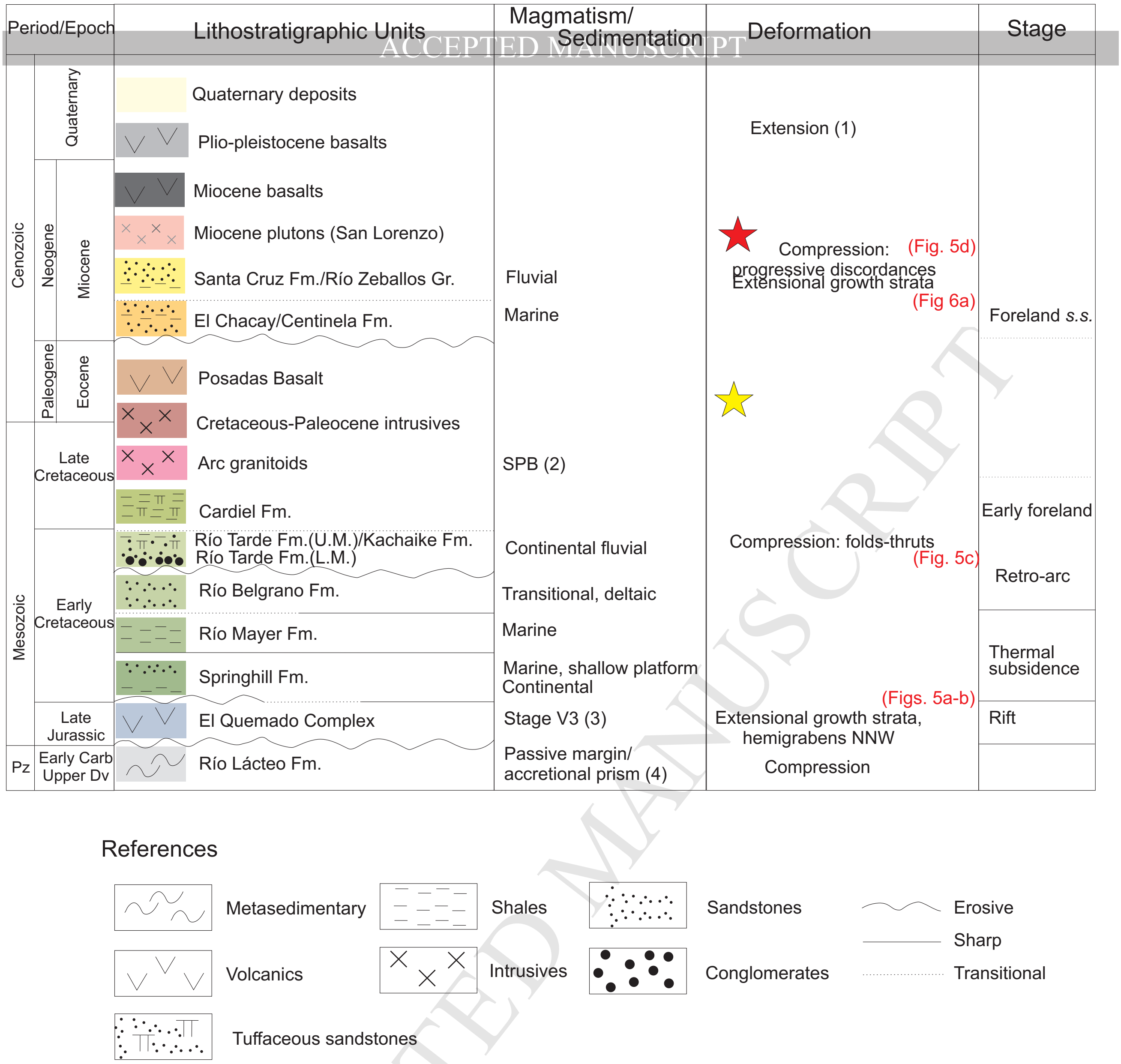
Period/Epoch
Lithostratigraphic Units
Magmatism/ Sedimentation
Deformation
Stage
Cenozoic
Neogene
Paleogene
Quaternary
Miocene
Eocene
Mesozoic
Late Cretaceous
Early Cretaceous
Late Jurassic
Pz
Early Carb Upper Dv
Quaternary deposits
Plio-pleistocene basalts
Miocene basalts
Miocene plutons (San Lorenzo)
Santa Cruz Fm./Río Zeballos Gr.
El Chacay/Centinela Fm.
Posadas Basalt
Cretaceous-Paleocene intrusives
Arc granitoids
Cardiel Fm.
Río Tarde Fm.(U.M.)/Kachaike Fm.
Río Tarde Fm.(L.M.)
Río Belgrano Fm.
Río Mayer Fm.
Springhill Fm.
El Quemado Complex
Río Lácteo Fm.
Fluvial
Marine
SPB (2)
Continental fluvial
Transitional, deltaic
Marine
Marine, shallow platform
Continental
Stage V3 (3)
Passive margin/
accretional prism (4)
Extension (1)
Compression: (Fig. 5d)
progressive discordances
Extensional growth strata
(Fig 6a)
Compression: folds-thruts
(Fig. 5c)
(Figs. 5a-b)
Extensional growth strata,
hemigrabens NNW
Compression
Foreland s.s.
Early foreland
Retro-arc
Thermal subsidence
Rift
References
Metasedimentary
Shales
Sandstones
Erosive
Sharp
Transitional
Volcanics
Intrusives
Conglomerates
Tuffaceous sandstones

FIGURE 9

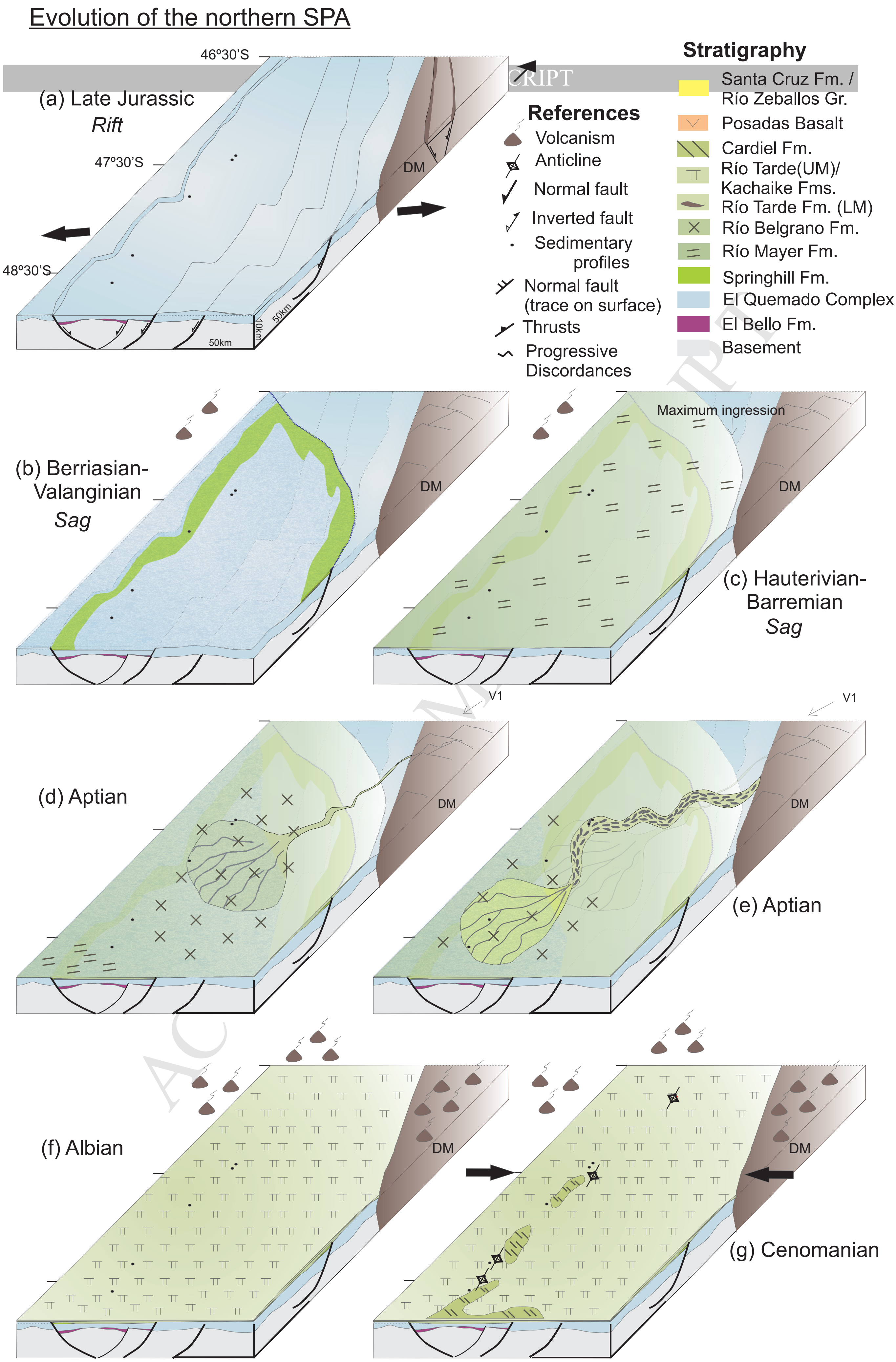

Evolution of the northern SPA
46°30'S
47°30'S
48°30'S
(a) Late Jurassic
Rift
DM
10km
50km
50km
(b) Berriasian-
Valanginian
Sag
Maximum ingression
(c) Hauterivian-
Barremian
Sag
(d) Aptian
V1
(e) Aptian
(f) Albian
(g) Cenomanian
References
Volcanism
Anticline
Normal fault
Inverted fault
Sedimentary profiles
Normal fault (trace on surface)
Thrusts
Progressive Discordances
Stratigraphy
Santa Cruz Fm. / Río Zeballos Gr.
Posadas Basalt
Cardiel Fm.
Río Tarde(UM)/ Kachaike Fms.
Río Tarde Fm. (LM)
Río Belgrano Fm.
Río Mayer Fm.
Springhill Fm.
El Quemado Complex
El Bello Fm.
Basement

FIGURE 10

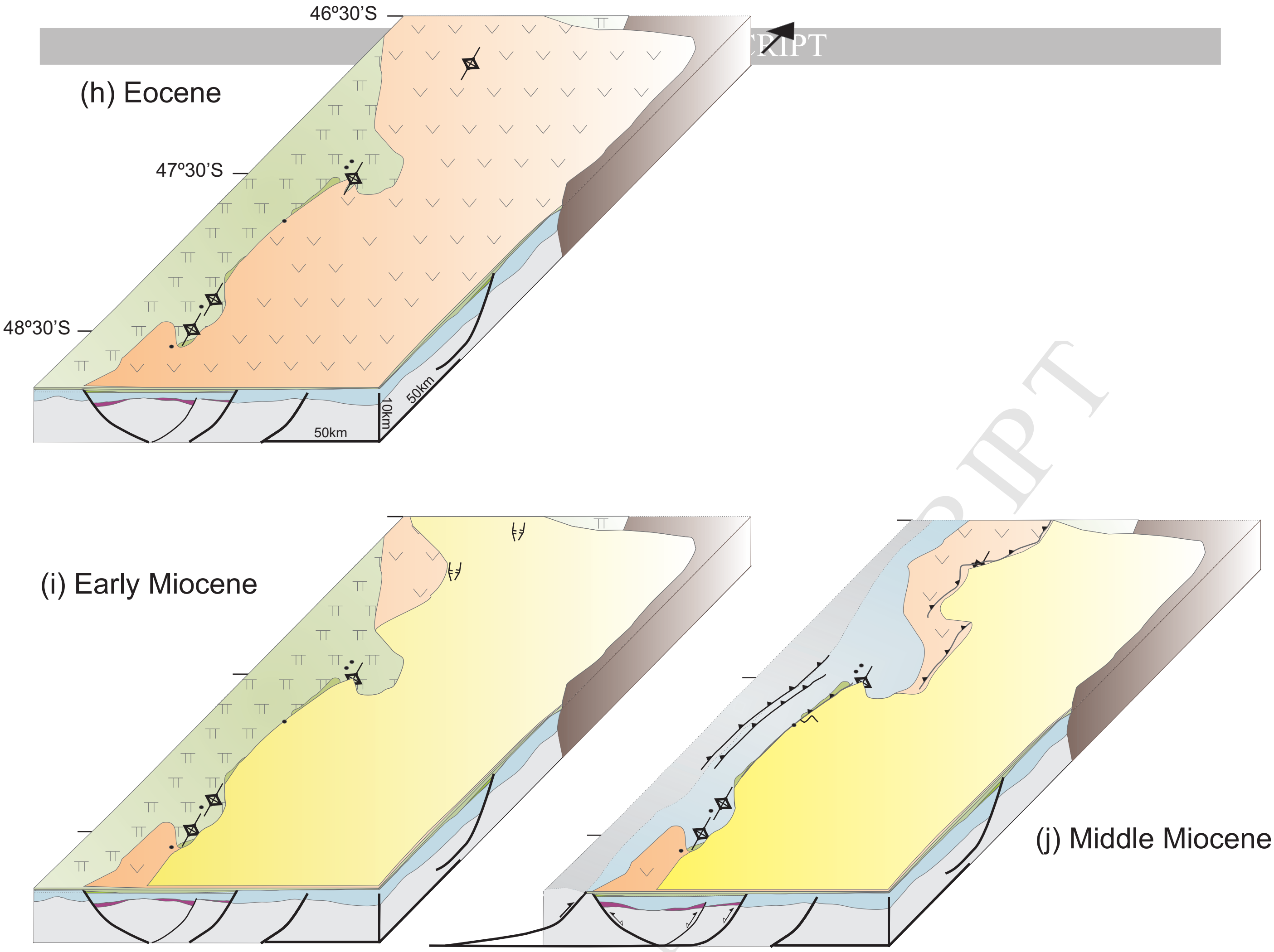

46°30'S
(h) Eocene
47°30'S
48°30'S
50km
10km
50km
(i) Early Miocene
(j) Middle Miocene

FIGURE 10

Highlights:

An integrate study allow us to unravel the different deformational events that took place in the area linked to variable regional geodynamic contexts.

We propose an evolution model for the northern sector of the Southern Patagonian Andes and define four tectonostratigraphic stages.

A major change in the provenance pattern is detected between Cretaceous and Cenozoic rocks.